AD-A040 932 NAVAL SURFACE WEAPONS CENTER WHITE OAK LAB SILVER SP--ETC F/G 20/5
CONDENSED FUELS FOR HIGH ENERGY GAS DYNAMIC LASERS.(U)
AUG 76 G B WILMOT, E G POWELL, H S HAISS

UNCLASSIFIED NSWC/WOL-TR-77-51 NL

| OF |
AD
A040 932

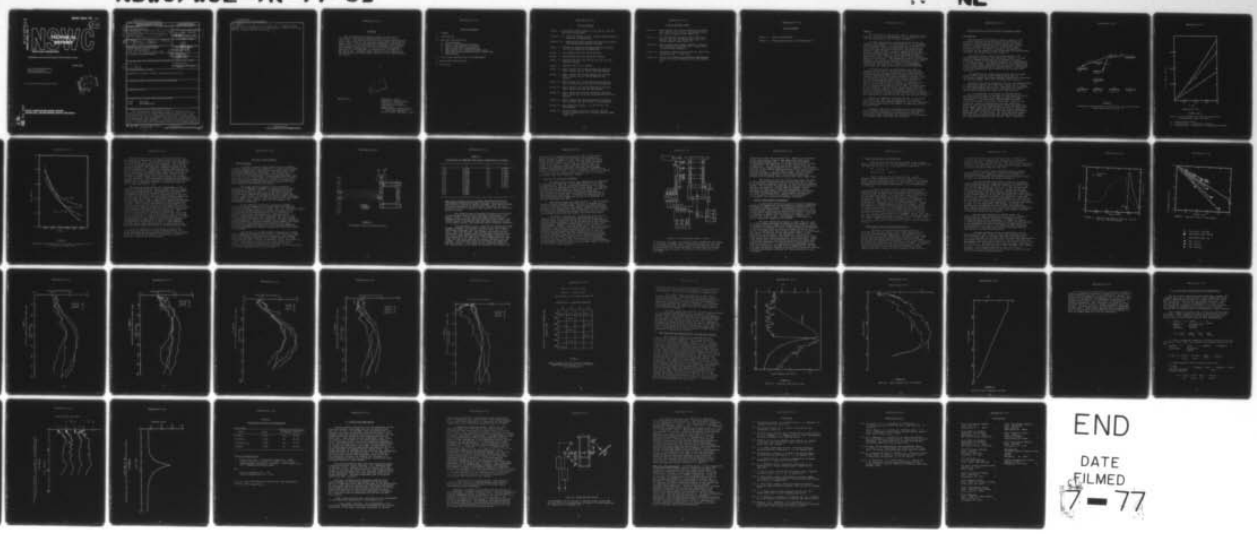

END
DATE FILMED
7-77

NSWC/WOL/TR 77-51

NSWC TECHNICAL REPORT

WHITE OAK LABORATORY

CONDENSED FUELS FOR HIGH ENERGY GAS DYNAMIC LASERS

AUGUST 1976

NAVAL SURFACE WEAPONS CENTER
WHITE OAK LABORATORY
SILVER SPRING, MARYLAND 20910

- Approved for public release; distribution unlimited.

NAVAL SURFACE WEAPONS CENTER
WHITE OAK, SILVER SPRING, MARYLAND 20910

UNCLASSIFIED

SECURITY CLASSIFICATION OF THIS PAGE *(When Data Entered)*

REPORT DOCUMENTATION PAGE

READ INSTRUCTIONS BEFORE COMPLETING FORM

1. REPORT NUMBER: NSWC/WOL-TR-77-51	2. GOVT ACCESSION NO.
3. RECIPIENT'S CATALOG NUMBER	
4. TITLE *(and Subtitle)*: Condensed Fuels for High Energy Gas Dynamic Lasers.	5. TYPE OF REPORT & PERIOD COVERED: Final report - Ending June 1976
6. PERFORMING ORG. REPORT NUMBER	
7. AUTHOR(s): G. B. Wilmot, E. G. Powell, H. S. Haiss, R. C. Gill and O. H. Dengel	8. CONTRACT OR GRANT NUMBER(s)
9. PERFORMING ORGANIZATION NAME AND ADDRESS: Naval Surface Weapons Center, White Oak Laboratory, White Oak, Silver Spring, Maryland 20910	10. PROGRAM ELEMENT, PROJECT, TASK AREA & WORK UNIT NUMBERS: 61153N; WR02403 WR0240301 WR2912;
11. CONTROLLING OFFICE NAME AND ADDRESS	12. REPORT DATE: August 1976
	13. NUMBER OF PAGES: 43
14. MONITORING AGENCY NAME & ADDRESS *(if different from Controlling Office)*: 51 p.	15. SECURITY CLASS. *(of this report)*: UNCLASSIFIED
	15a. DECLASSIFICATION/DOWNGRADING SCHEDULE

16. DISTRIBUTION STATEMENT *(of this Report)*

Approved for public release; distribution unlimited

17. DISTRIBUTION STATEMENT *(of the abstract entered in Block 20, if different from Report)*

18. SUPPLEMENTARY NOTES

19. KEY WORDS *(Continue on reverse side if necessary and identify by block number)*

Fuels
Laser
Solid Fuel
Gas Dynamic Laser

20. ABSTRACT *(Continue on reverse side if necessary and identify by block number)*

The conventional gas dynamic laser is driven by a gas mixture consisting of approximately 85% N_2, 10% CO_2 and 5% H_2O. The formulation of all solid fuels which generate such a gas mixture at the required temperatures and rates is beyond reach. Investigations were conducted to determine the small signal gain of gas compositions amenable to all solid gas generator formulating. It was found that acceptable gains can be achieved when N_2

DD FORM 1 JAN 73 1473 EDITION OF 1 NOV 65 IS OBSOLETE
S/N 0102-014-6601

UNCLASSIFIED
SECURITY CLASSIFICATION OF THIS PAGE *(When Data Entered)*

391 596

20. (cont)
is partically replaced by CO and H_2O by HCl. Based on these results a solid composition was formulated and tested which gave 28% CO, 10% CO_2, 16% HCl and 46% N_2.

ABSTRACT

The conventional gas dynamic laser is driven by a gas mixture consisting of approximately 85% N_2, 10% CO_2 and 5% H_2O. The formulation of all solid fuels which generate such a gas mixture at the required temperatures and rates is beyond reach. Investigations were conducted to determine the small signal gain of gas compositions amenable to all solid gas generator formulating. It was found that acceptable gains can be achieved when N_2 is partically replaced by CO and H_2O by HCl. Based on these results a solid composition was formulated and tested which gave 28% CO, 10% CO_2, 16% HCl and 46% N_2.

Approved by:

THEODORE D. AUSTIN
Propellant Physics Branch
Propellants Division
Research and Technology Department
NAVAL SURFACE WEAPONS CENTER
WHITE OAK LABORATORY
Silver Spring, Maryland 20910

List of Contents

List of Figures

List of Figures (cont)

List of Tables

Summary:

The conventional gas dynamic laser is driven by a gas mixture consisting of approximately 85% N_2 (pumping gas), 10% CO_2 (working gas) and 5% water (relaxant).

For many applications, the practicality of the gas dynamic laser depends on the availability of non-cryogenic condensed phase fuels. If such liquid or solid fuels are to be realized, careful consideration must be given to relaxation catalysts other than water and pumping gases different from nitrogen. A small laboratory-scale gas dynamic combustion laser has been assembled and applied to the study of the effects of lasing gas compositions on small-signal gain. The device can burn 5 to 10 grams of gaseous or solid fuel. The combustion products are expanded through a slit nozzle of expansion ratio 50:1 into a test region where small-signal gain can be simultaneously measured at four positions. Useful gain measurements can be made for times of the order of 100 milliseconds.

An extensive series of measurements were made to determine the effect on small-signal gain of replacing portions of the nitrogen content of the product gases by carbon monoxide and substituting hydrogen chloride and hydrogen fluoride for the usual relaxation catalyst, water. The results on the HCl-containing mixtures showed that HCl performed somewhat better than a H_2O-containing mixture of the same relaxant content. In addition, the gain of CO-containing mixtures decreases less rapidly with increasing CO-content if HCl is used instead of water as the relaxant. The HF studies showed good performance to quite high HF-contents in N_2-pumped mixtures but the gain in mixtures containing CO was low compared to similar mixtures with HCl. Based on these results, a solid composition was formulated to give 28% CO, 10% CO_2, 16% HCl, and 46% N_2.

Because of combustion problems the gain of the solid formulation was less than that measured for a gaseous fuel giving the same product composition but the formulation did indicate that useful performance is achievable with an all-solid fuel.

Recently, the mixing gas dynamic laser has received great attention because of its potential for considerably higher specific performance characteristics over the conventional GDL. Techniques for measuring the performance of candidate MGDL fuels have been analyzed.

Condensed Fuels for High Energy Gas Dynamic Lasers

Introduction:

The conventional gas dynamic laser is based on the stimulated emission of photon energy by $N_2/CO_2/H_2O$ gas mixtures. The conversion of thermal energy into photon energy is achieved through energy transfer from the hot two level energy carrier gas, N_2, to the three level working gas, CO_2. In order to maintain the population inversion, H_2O is added in small percentages for deactivating the lower CO_2 energy levels (see Figure 1).

The energy carrier gas N_2 can store energy in its translational, rotational and vibrational states. In each degree of freedom (fully excited) a molecule can store an average of 1/2 kT of energy (rotational or translational) or kT (vibrational). The energy stored in the translational and rotational modes increases linearly with kT, whereas the linear energy relationship for the vibrational states begins to hold at temperatures above 1000°K as can be seen from Figure 2(a).

The equilibration of the translational and rotational energy levels of N_2 at 2000°K requires only about 5 collisions, whereas for energy exchange between the vibrational and external modes, about 10^6 collisions are required.

Because of the large relaxation time for the thermalization of vibrational energy, the vibrational energy can be frozen by rapid expansion of hot N_2 gas. Basically it is the frozen N_2 vibrational energy which can be converted into photon energy after transfer to a three level working gas.

It is instructive to calculate the maximum energy available per unit mass of nitrogen for CO_2 lasing at 10.6μm. This can be done easily if we assume a simplified model (reference 1). In this model, the available nitrogen vibrational energy is the total vibrational energy at the vibrational freezing temperatures less the vibrational energy at that nitrogen temperature at which the population of the upper (001) CO_2 level is equal to that of lower (100) level. The results of such calculations of the available energy are shown in Figure 2(b) for the harmonic oscillation approximation. In this figure, the total available energy from unit mass of nitrogen has been multiplied by 0.409, the quantum efficiency of the 10.6μm laser transition.

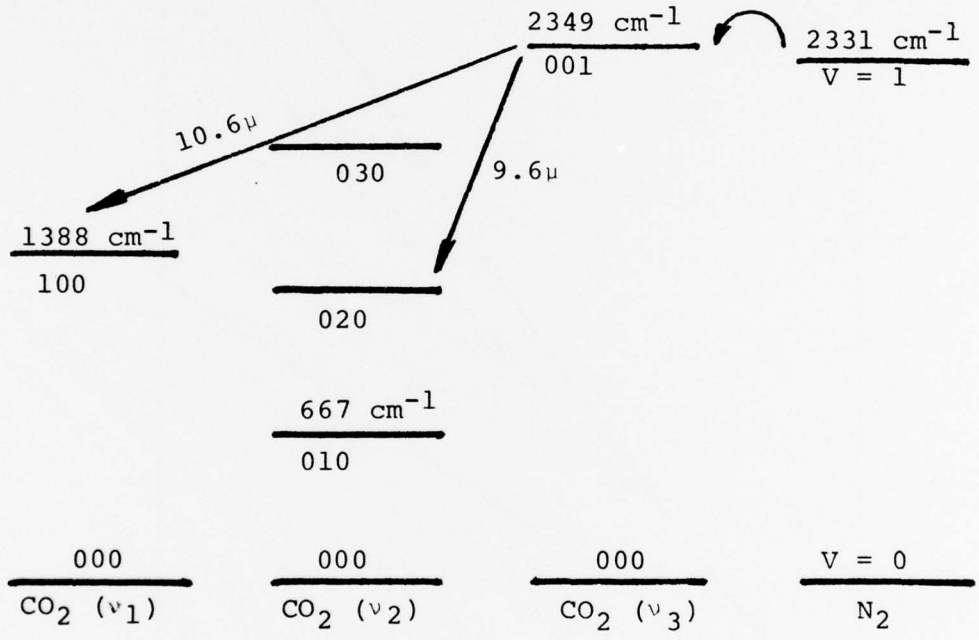

Figure 1

Vibrational Energy Levels in CO_2 and N_2, and the CO_2 Laser Transitions (see e.g. ref. 1)

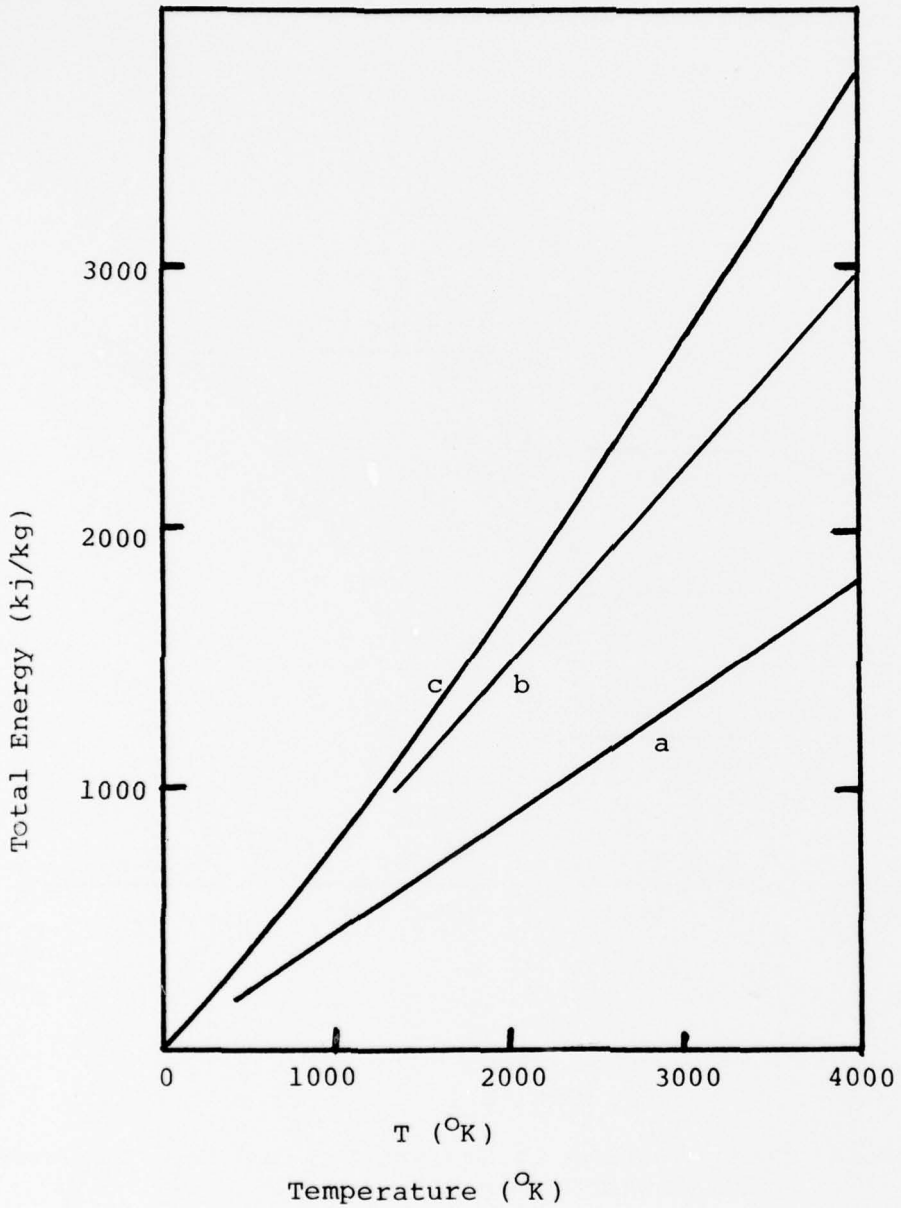

Temperature (°K)

Figure 2 (a)

Energy of N_2 in Thermal Equilibrium as Function of Temperature (see e.g. Ref. 2)

a. Translational energy
b. Translational + rotational energies
c. Translational + Rotational + vibrational energies

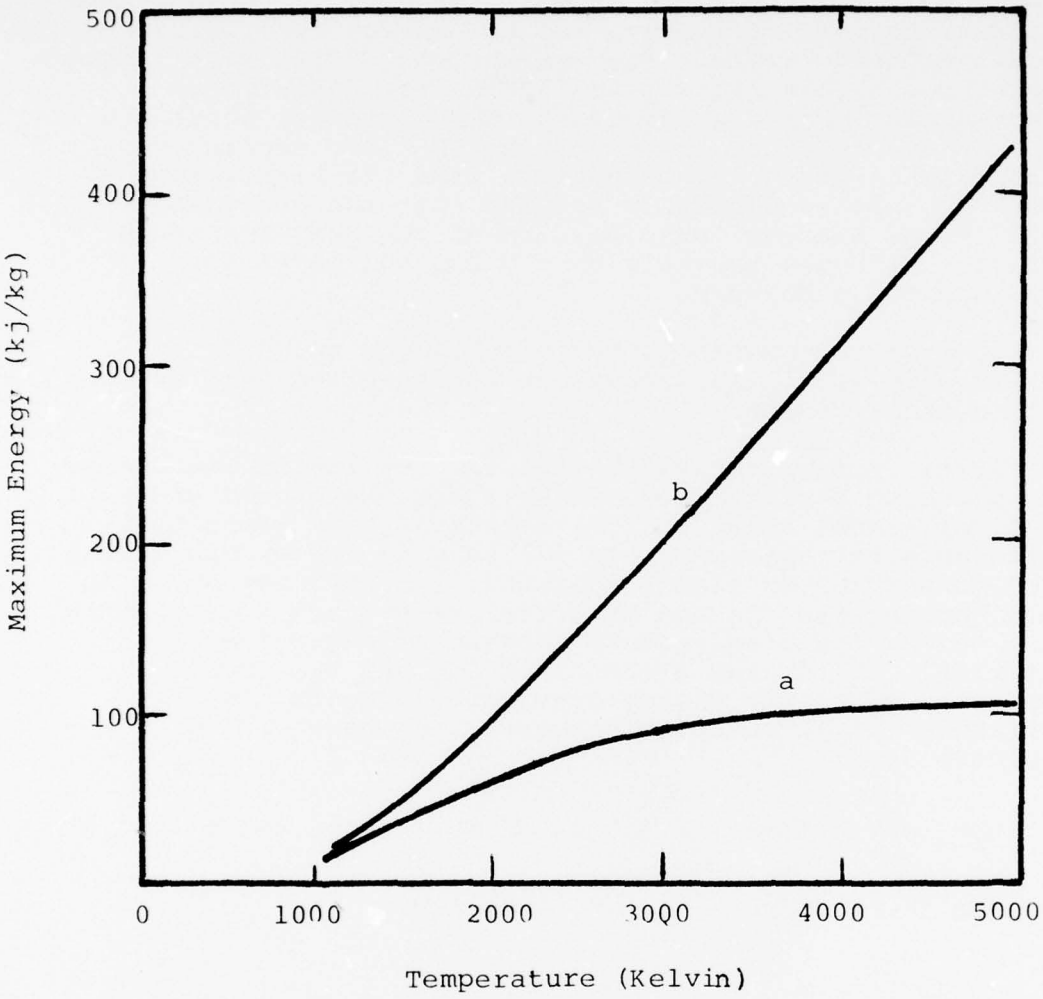

Figure 2 (b)

Maximum Available Energy for 10.6μm CO_2 Lasing From Vibrationally Excited Nitrogen

a. From first level
b. From all levels

The energy is shown for two cases: energy contributions from the first excited level only, and the energy contribution from all excited levels. For conventional GDL's with freezing temperatures in the range 1000-1500°K, the differences are not great. For high freezing temperatures, which may obtain in devices such as the mixing GDL (see Section V), the importance of the contributions from the higher levels is obvious. It is generally assumed that the energies of all levels are available because of the near resonance of all the nitrogen levels with the CO_2 001 level for single quantum exchanges.

The critical question, however, is how much of the theoretically available energy can be converted into photons in a practical device.

First, it is a necessity that the CO_2 lasing transition takes place to a vibrational state above the ground state. This lower -level energy ultimately appears as waste heat and accounts for approximately 60% loss in frozen vibrational energy conversion to laser radiation. Second, the addition of the working gas CO_2 and the relaxant H_2O has a detrimental effect on the freezing process because of their faster relaxation. Third, the presence of CO_2 and H_2O, even though the key to the energy conversion process, leads to undesirable energy transfer processes, as shown below (reference 3).

$$N_2^* \text{ (or } CO_2(001)) + H_2O \longrightarrow N_2 \text{ (or } CO_2 \text{ (000))} + H_2O \quad (1)$$

$$CO_2(001) + CO_2 \longrightarrow CO_2(100) + CO_2 \quad (2)$$

$$CO_2(001) + N_2 \longrightarrow CO_2(100) + N_2 \quad (3)$$

These energy transfer (thermalization) processes partially deactivate the excited N_2 levels in the nozzle before the power extraction section. These deactivation processes are detrimental to the laser performance and become more pronounced with higher temperatures as shown in Figure 3 (reference 3). In fact, it is the deactivation processes, 1-3, which prohibit operation of a $N_2/CO_2/H_2O$ laser at higher temperatures.

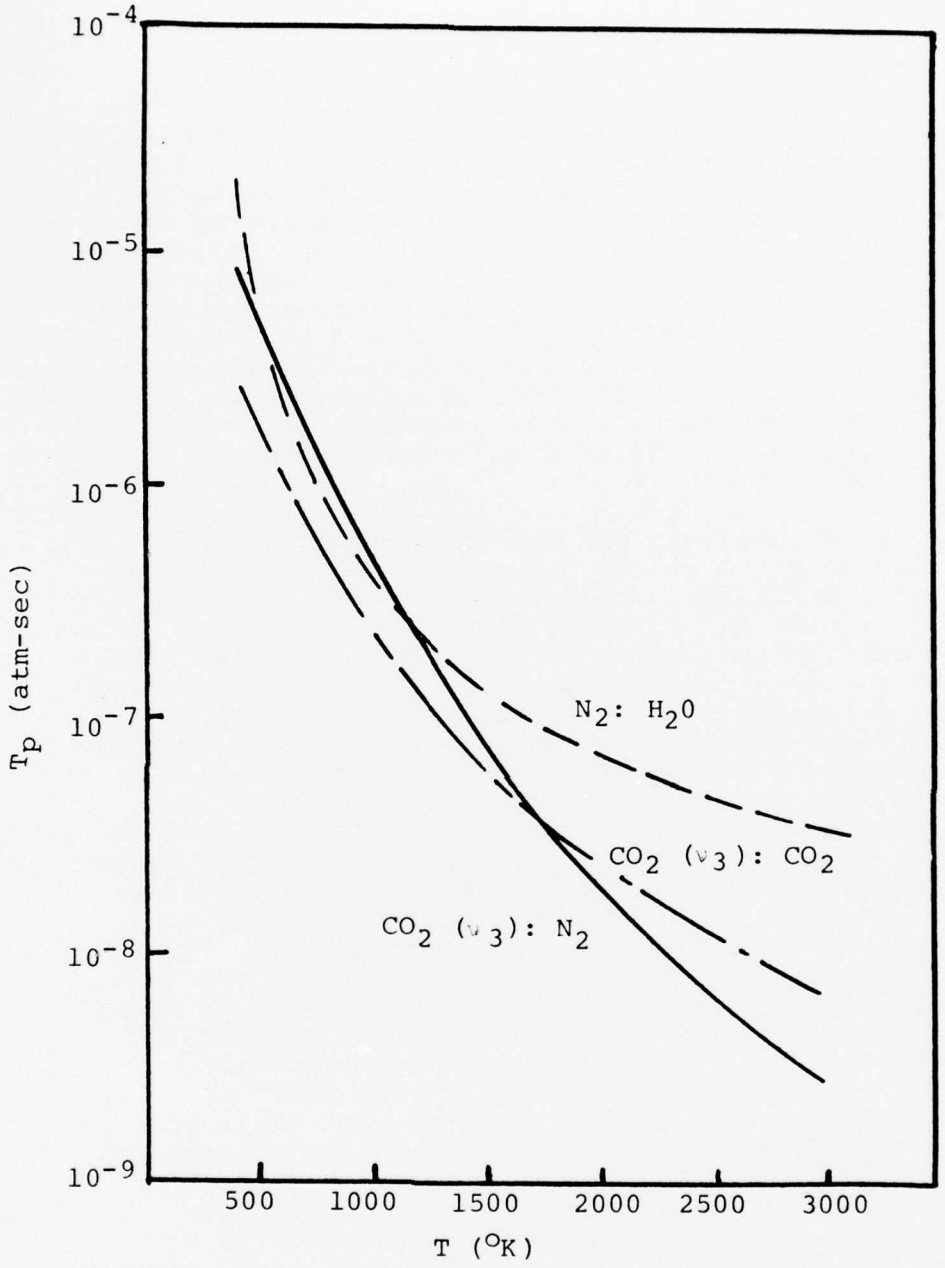

Figure 3

Relaxation Times For The Deactivation Processes (1)-(3) as Function of Temperature

More efficient use of the N_2 vibrational energy can be achieved by separating the energy carrier gas, N_2, from the working gas, CO_2. This scheme requires the injection of CO_2 into the N_2 gas stream after expansion. Early efforts to use this scheme suffered from inadequate mixing of the two gas streams in the supersonic expansion region of the nozzle (reference 4). According to recent publications use of a screen nozzle can remedy this difficulty (reference 3). Thus, the mixing gas dynamic laser (MGDL) appears to be an attractive concept with the potential for a 3 to 5 fold increase in power output over a conventional GDL per mass unit of reactants. This performance increase can be achieved because the N_2 can now be heated to temperatures as high as $4000^{o}K$ with a subsequent increase in stored N_2 energy as can be seen from Figure 2 (b).

For practical applications the replacement of the cryogenic liquids N_2,CO and O_2 by storable solid or liquid fuels is highly desirable. Unfortunately, the replacement of cryogenic liquids by storable fuels is faced with fundamental difficulties which stem directly from the high nitrogen and low water vapor and carbon dioxide contents of the required gas mixture. A gas generator formulation with the empirical formula $C_3H_2O_7N_{32}$ is required to generate the gas composition: 80% nitrogen, 15% carbon dioxide and 5% water. Such an empirical formula for the product gas requires every major ingredient in the formulation to be a high nitrogen compound or that the formulation retain large and undesirable amounts of solid residues, as it would be required for sodium azide based gas generators. The partial substitution of the energy carrier gas, N_2, by CO and of the deactivant, H_2O by HCl may be a way to overcome these difficulties. A number of promising studies in other laboratories have been made in shock-tube GDL systems on the dependence of small-signal gain on carbon monoxide concentration (references 5, 6, and 7). The NSWC/WOL and AFWL groups have used helium as a relaxant while the Math Sciences studies used water at various concentrations.

It is the objective of this effort to search for acceptable gas mixtures with partial substitution of N_2 by CO and of H_2O by HCl or HF since the use of these product gases will make the achievement of practical solid gas generator formulations more probable.

GDL Fuel Testing Device

1. Design Concept:

In order to measure small-signal gain for gaseous products resulting from the combustion of either gas mixtures or solid formulations, a laboratory-scale gas dynamic laser system was designed and constructed. The inspiration for this design derives partially from the shock-tube GDLs (see e.g. ref. 8) and partially from the explosion-type GDL's (see ref. 9,10,11). Both types have demonstrated that useful small-signal gain measurements can be made in systems with short (millisecond) running times which require relatively small amounts of the lasing gas mixture.

The basic device assembled at this laboratory consists of a combustion chamber, an expansion nozzle and a gain-measuring section (Fig. 4). To minimize corrosion problems, all parts are made of type 304 stainless steel. The cylindrical combustion chamber,102mm long x 127mm dia., volume = 1.287 liters, is designed to contain 17MPa (2500 psi) with an ample safety factor. The cylinder head of the chamber contains ports for igniter leads and for pressure and temperature transducers.

At the opposite end of the cylindrical chamber a plate connects the chamber to the nozzle via a rectangular aperture of volume 15.2 x 127 x 25 mm = 48.3 ml. This small volume is isolated from the combustion chamber and nozzle by two brass rupture diaphragms 0.1mm thick, and is connected to pressurizing and venting systems via a solenoid valve. Before an experiment, two brass diaphragms, scored to break cleanly without fragments, are installed. The small volume is pressurized with nitrogen to about half the peak combustion pressure expected. After the mixture in the chamber is ignited and reaches its peak pressure, the solenoid valve opens, releasing the supporting pressure on the upstream diaphragm. The two diaphragms then rupture and admit the combustion gases to the nozzle.

The nozzle is a minimum-length contoured slit nozzle with a geometric expansion ratio of 60:1. The throat is .36mm high by 127mm long. The radius of curvature in the subsonic region just upstream from the sharp corner throat is 0.36mm which satisfies the criterion of Greenberg et al (references 18, 19) that this radius be small-of the order of the throat height. The profile was specifically designed for high performance GDL use by the Aerodynamics Branch of this laboratory. The nozzle coordinates are given in Table I.

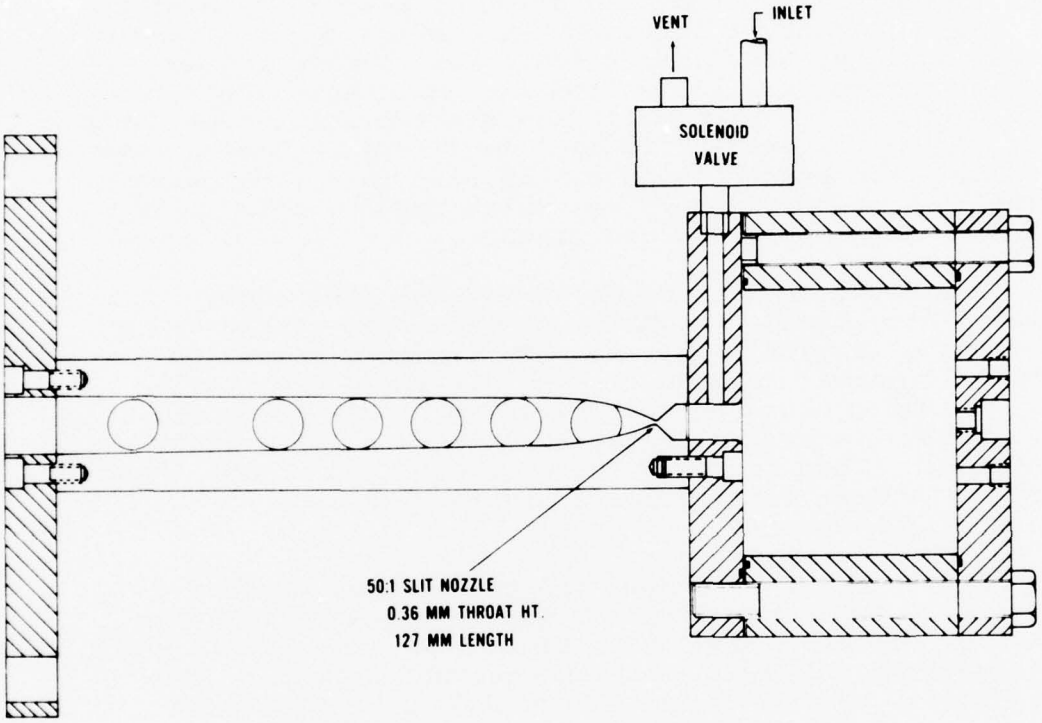

Figure 4

Gas Dynamic Laser For Fuels Testing

Table I

Coordinates for NSWC/WOL GDL Nozzle (Dimensions in Inches)

X	Y	X	Y
0.0	0.0070	0.9	0.2931
0.01	0.0160	1.0	0.3083
0.02	0.0248	1.1	0.3222
0.05	0.0475	1.2	0.3349
0.1	0.0770	1.3	0.3466
0.15	0.1017	1.4	0.3572
0.2	0.1220	1.5	0.3668
0.25	0.1408	1.7	0.3835
0.3	0.1580	1.9	0.3973
0.35	0.1739	2.0	0.4033
0.4	0.1886	2.4	0.4214
0.45	0.2022		
0.55	0.2265		
0.65	0.2480		
0.8	0.2769		

The nozzle contour and the slightly divergent downstream sections were ground from single stainless steel plates for each half by a precision contour grinder. This design feature avoids the generation of shock waves created by the small discontinuity which results at the juncture when two separate pieces are used.

The nozzle plates are bolted to plates at both ends and bolted and pinned to two 25mm thick side plates. The proper aligment of the upper and lower throat sections depends on the precision of the grinding of the parts. The throat height is determined when the side plates are pinned to the nozzle plates, and cannot be easily adjusted thereafter.

Six observation ports which can be fitted with 25mm diameter windows, are located in each of the side plates at downstream distances from the throat of 28.2, 66.3, 104.4, 142.5, 180.6 and 250.4mm. The windows are sealed against 1.5mm thick flat Teflon gaskets by threaded retaining rings. The inner window surfaces are recessed about 4mm below the inner surface of the side walls. The windows could be made flush with the wall surfaces by cutting shoulders into the windows. This operation would be difficult and expensive and was not done. The effect of the recessed windows on the flow pattern is not known but presumed to be minor and

confined to the immediate vicinity of these lateral walls. After leaving the observation region, the expanded gas passes through a 166mm i.d. gate valve and pipe (the total length of this 166mm i.d. section is .75m) before entering a dump tank .56m i.d. diam x 2.1m long total volume ∿590 liters. Gas samples can be withdrawn from the tank for infrared spectroscopic analyses. The tank can be pumped down to a pressure of 7Pa (0.05 Torr) through a 50mm diam pipe at the far end. A liquid nitrogen cooled trap in the line serves to remove corrosive gases before they reach the 25 liter/sec mechanical pump (Welch Model No. 1398M).

2. Optical Data Reduction Systems:

The small-signal gain of the expanded gas is measured by passing the output of a 3 watt Model 941 C.W. CO_2 laser through the gas. The 941, although performing fairly satisfactorily, is the dominant source of signal noise. In addition, occassionally abrupt drops in output occur which can persist for many tens of milliseconds, spoiling an experiment. These changes in output could be related to mode changes or rotational transition jumps. A stabilizing retrofit kit is now available for this laser and its use is recommended if further experiments are done.

The optical layout is shown in Fig. 5. The vertically polarized 10.6μm radiation from the laser is chopped at 2.1 kHz by a rotating 48 shot blade. The beam is then reflected parallel to the axis of the GDL system. Sodium chloride beam splitters, 80% transmission, 10% reflectivity for each surface for vertically polarized radiation, reflect portions of the beam through sodium chloride windows into the test volume.

The beam is returned by a gold-coated mirror on the opposite side. The incoming beam reflected from the beam splitter makes an angle of 12^{o} in the vertical plane with the returning beam to separate the beams about 6mm at the detectors. Gold mirrors, roughened to reduce sensitivity to small beam displacements, reflect the four beams up into the four detectors. Two types of detectors are used. Two are perovskite pyroelectric types (Laser Precision Model Nos. KT-4110 and KT-4205) and can withstand power densities of 10 and 100 watts/cm^2 respectively. The low reflectivities of the beam splitters and the transmission of the window/detector/mirror system limit the power to less than 0.5 watts at the most delicate detector. The other two detectors are gold-doped germanium photoconductors built into the small liquid-nitrogen cooled dewars. These detectors have response times of the order of 2 to 10μsec and have better

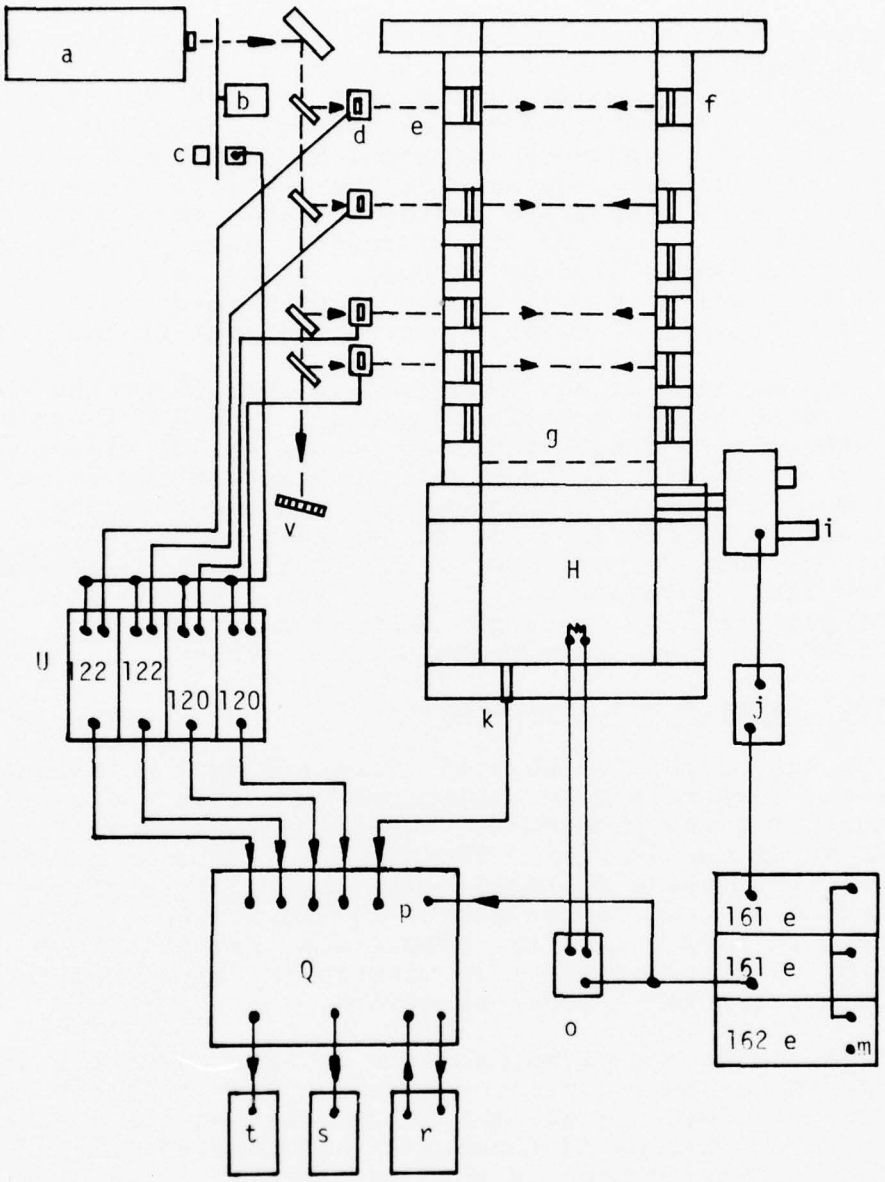

Figure 5: Four Channel Gain Measuring System

(a) 941 laser, (b) chopper, (c) reference signal, (d) detectors, (e) windows, (f) reflectors, (g) nozzle throat, (H) combustion chamber, (i) vent value, (j) vent relay switch, (k) pressure gauge, (l) pulse generator, (m) start pulse, (n) delay, (o) firing relay switch, (p) start signal, (Q) computer, (r) magnetic tape, (s) printer, (t) plotter, (U) lock-in amplifier, (v) bean stopper.

detectivities than the pyroelectrics. However at the signal levels and response times of the experiment, both types perform about equally well. The output of each detector is demodulated and amplified to the one volt level by a lock-in amplifier. The frequency and phase of the signal are referenced to a signal generated at the chopper. Non-uniform rotation of the chopper blade proved to be an annoying source of spurious signals in the 300 Hz range. This problem was partially solved by replacing the pulleys and belt of the chopper with some which give a more uniform rotational velocity and by special care in tuning the lock-in amplifiers.

The outputs of the four lock-in amplifiers and those of the pressure transducers are digitized at a 500 Hz rate by an analogue-to-digital converter in the PDP-8E minicomputer system. The raw data are acquired, printed out and stored on magnetic cartridge by a simple machine language routine. The data are read back in after the experiment is over, smoothed, and the pressure and small-signal gain calculated by a BASIC language program. This program can also plot curves of gain vs time or vs pressure on an attached x-y recorder via a digital-to-analogue converter.

3. Typical Experimental Procedures:

A gas mixture which will yield the desired combustion products and temperature as determined by a rocket propellant performance computer program is prepared manometrically in stainless steel gas bottles. The prepared mixtures are well-stirred before loading by oscillation and rotation of the gas bottles which contain Teflon pieces to aid mixing. Typically the mixture is loaded into the combustion chamber to a pressure of .5 MPa (5 atm). The mixture is formulated to give a combustion temperature of 1800^{o}K.

The peak combustion pressure is about 3MPa (30 atm) if no heat losses and complete combustion are assumed. After the mixture had been loaded, the volume between the diaphragms is loaded to a pressure of about 1/2 the expected peak pressure. It was found that ignition is more reliable if the hot wire igniter is augmented by coating with about 50mg of nitrocellulose. This amount of material has no appreciable effect on the composition of the gases. The ignition is initiated by a manually actuated trigger which fires the ignitor power supply relay switch and starts the computer data acquisition. After a selectable delay of 100-500 msec which has been determined by previous experience with the particular gas mixture, the venting solenoid valve is opened and the diaphragms rupture. After the experiment, the dump tank is pumped out through the cold trap and then the system is returned to atmospheric pressure to enable disassembly, cleaning and the installation of new diaphragms.

4. Small Signal Gain Considerations:

The small-signal gain has been taken to be the most useful figure of merit for the performance of a fuel composition. The small-signal gain, G_o, is defined by the equation:

$$\frac{dI}{I} = G_o\, dl \quad \text{or}$$

$$\ln I/I_o = Gl \qquad \text{(Ref. 1)}$$

where I and I_o are the signal levels at the detectors with and without the test gas in the path. The levels are both zero with respect to zero signal at zero probe laser intensity (beam blocked). dl and l are the path length increment and path length respectively. In our experiment, l = 25.4 cm.

In order to be defined as a small-signal gain, the measurement has to be done at low enough probe beam power levels so that the population distribution in the test gas is not appreciably altered. That the small signal condition is met in these experiments is evident by the following calculation. The beam power in the test gas is estimated to be about 0.1 watts. At a gain of 1/meter, this power is increased by $\sim$.029 watts or 1.5×10^{18} photons/sec. The gas flow rate at a chamber pressure of 20 atm is about 2×10^{24} molecules/sec, or across the 5mm height of the beam, about 4×10^{23} molecules/sec. At an assumed freezing temperature of 1500°K and at assumed CO_2-N_2 vibrational equilibrium the relative population of the 001 level is about 0.1, or about 6×10^{21} CO_2 (001) molecules/sec. The number of CO_2 (001) $\longrightarrow$ CO_2 (100) transitions is only 1.5×10^{18}/sec. Thus, the number of CO_2 (001) molecules affected is about 2.5×10^{-4} of the total (6×10^{21}) upper laser level CO_2 population. It can be seen that small-signal gain conditions will hold to quite low chamber pressure.

5. Experiments With Premixed Gaseous Fuels:

Generally, fuel mixtures have been made up of nitrogen, CO, O_2, N_2O and H_2 in the proper proportions to give desired resulting composition. The O_2/N_2O ratio is adjusted to give a flame temperature of 1800°K as calculated by our rocket propellant performance computer program. For the 4% HCl-containing combustion gases, the HCl is formed by addition of chloroform and hydrogen in the proper proportions. For higher HCl concentrations HCl itself is added. To generate various concentrations of HF, perfluorobutene-2, C_4F_8, is added to the fuel in the appropriate concentration with enough hydrogen to convert all the fluorine to HF. Hydrogen

is a desired component in any mixture up to ~10 mole % as it aids ignition and combustion. Above 10% H, the mixture tends to detonate. Halogen content makes ignition more difficult and slows on burning rate. For most fuels, combustion is better than 90% complete as determined by infrared analysis of the gas collected from the dump tank.

Figure 6 shows typical pressure and gain versus time curves, in this case for a rather slow burning HCl-containing mixture. Mixtures containing no halogen or relatively high hydrogen concentrations achieve peak pressure in about 1/2 the time of the curve of Figure 6.

The measurements were made on a series of gaseous fuels formulated to give combustion product gas compositions in the ranges 20-80% N_2, 0-70% CO, 5-15% CO_2, 0-15% HCl and 0-8% H_2O at 1800-2000^{o}K and 20-40 atm. A gas mixture which burns at 30 atms and 1800^{o}K to give a 80% N_2, 16% CO_2 and 4% H_2O product gas have been used as a comparison standard. In N_2/CO_2 mixtures, HCl gives somewhat higher gains than the water-relaxed mixtures of the same concentration. This finding confirms, in combustion mixtures, the results of shock tube studies (Ref. 12,13). Our gain measurements as a function of HCl concentration show a more rapid decrease of gain with HCl content than the shock tube experiments. A possible explanation is that, in our experiments, the burning rate seems to decrease with increasing chlorine content thus permitting more cooling and possibly also causing less complete combustion. These effects would result in a more rapid apparent decrease in gain with increasing HCl content.

As has been realized for several years, the substitution of carbon monoxide for some of the nitrogen in GDL gas mixtures greatly increases the number of fuel ingredients which can be considered. A number of studies in other laboratories have been done in shock-tube GDL systems on the dependence of small-signal gain on carbon monoxide concentrations (Ref. 5,6,7). The NSWC and AFWL groups have used helium as a relaxant while the Math Sciences studies used water at various concentrations.

Our most extensive series of experiments with CO have been at 10% HCl. Figure 7 shows the variation of gain with CO content for the mixtures that have been measured. It can be seen that, at 10% HCl, the gain falls off significantly more slowly than with other relaxants. We have made only one measurement with water which was at 2.7% H_2O and a $CO/(CO + N_2) + N_2$ ratio of .3. The gain for this case was about .8 of that of a 0% CO fuel and thus similar to the 1.0% water data of Math Sciences. For mixtures with only 4% HCl, the rate of decrease in gain with increasing CO content is about the same as for a 4% water-catalyzed mixture.

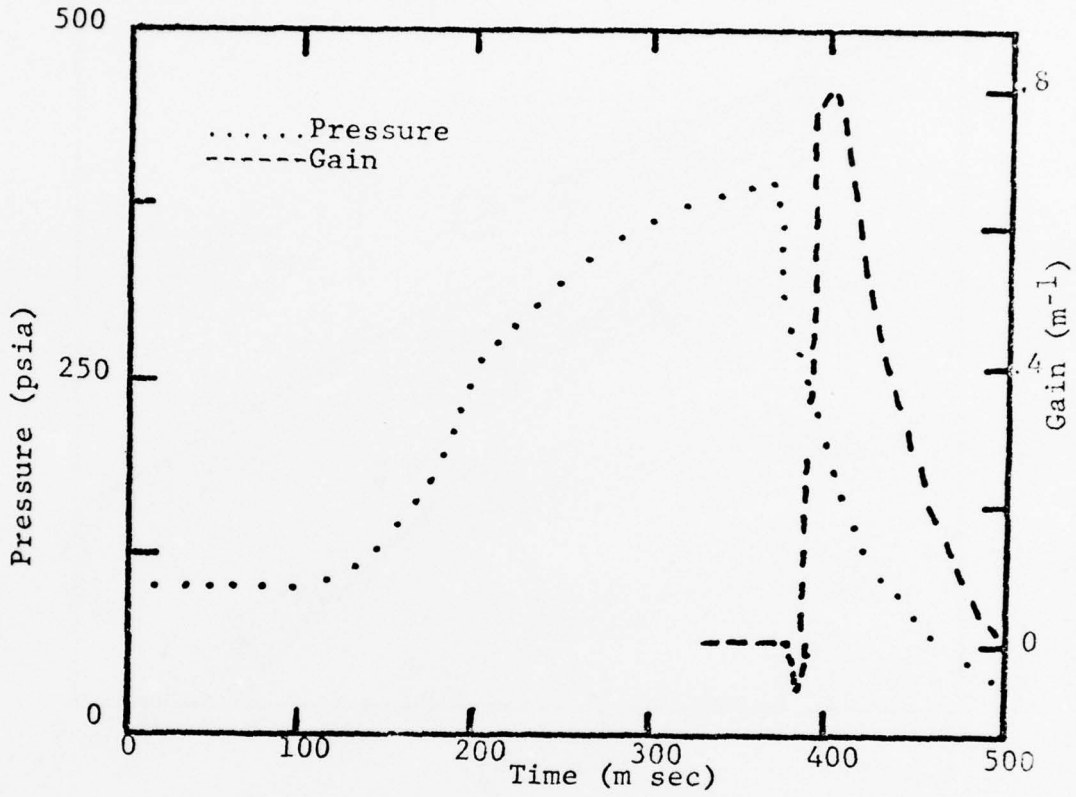

FIGURE 6: Pressure and Gain For 50% N_2, 25% CO, 15% CO_2, 10% HCl Mixture

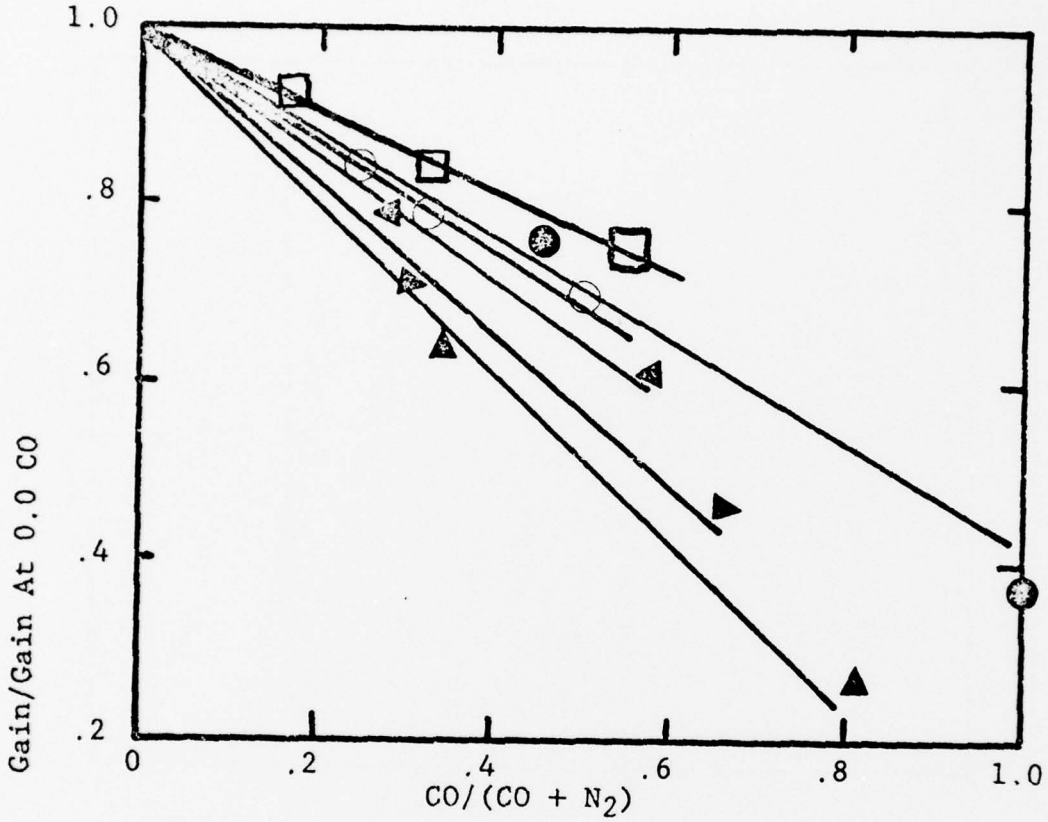

FIGURE 7: Relative Gain vs. CO Content

□ This work - 10% HCl

● NOL Shock Tube, 39% He

○ AFWL Shock Tube, He

◀ MSN, 1% H_2O

▶ MSN, 5% H_2O

▲ MSN, 10% H_2O

The effect of hydrogen fluoride on GDL performance is of considerable interest since a variety of attractive fluorine-containing condensed-phase candidate fuel ingredients are available. A series of tests at 4%, 12% and 15% HF have been done (Figures 8, 9 and 10) and can be compared to the standard 4% H_2O, 16% CO_2 and 80% N_2 mixture (Figure 11). In these figures, we have plotted measured gain as a function of chamber pressure. These plots are a particularly useful gauge of fuel performance in our system where the pressure is a decreasing function of time. The numbers on these curves refer to the four measurement positions downstream from the nozzle, No. 1 being closest (6.6cm) to the throat. Two important conclusions can be drawn from these data. Comparing Figures 8 and 9, we note that the 12% HF mixture gives a considerably higher gain than the 4% HF mixture. The 12% HF shot shows somewhat less peak gain (.7/m) than a comparable 10% HCl shot (.8/m) but peak gain (.5/m) for the 4% HF shot is quite low compared to that of a typical 4% HCl mixtures (1.0/m).

We have also done experiments on HF in combination with CO. As Figures 12 and 13 show in comparison to Figure 10 the CO in combination with HF lowers the gain considerably in comparison with HCl and CO mixtures.

We also note (Figure 9) that the gain at the second window (10.4 cm downstream from the throat) is higher than at the first. Most mixtures show a linear or quasilinear decrease of gain with downstream distances (Figure 10). Both these observations suggest that HF is a less efficient relaxant for the lower CO_2 level than either HCl or water. Thus, the slower relaxation rate gives peak output farther downstream and higher gain at higher concentrations. Further work is needed to find the optimum HF concentration and to test the performance of HF-catalyzed mixtures which contain carbon monoxide as a partial replacement for nitrogen as a GDL pumping gas.

As an attempt to compare all of these data we include a Table (Figure 14) summarizing the one-hundred or so shots we have done with various mixtures. The table entries are the peak gain in channel 1 and are in units of $meter^{-1}$. The entry preceding a solidus is for HCl-relaxed mixtures. The succeeding entry is for HF-relaxed mixtures. An x or a blank means no data are available. Most entries represent weighted averages of two or more shots. Low values of gain were given lower weight on the grounds that combustion inefficiency always lowers the gain compared to a completely burned mixture. Consequently, the true gain forms an upper bound for the measured gain plus uncertainties.

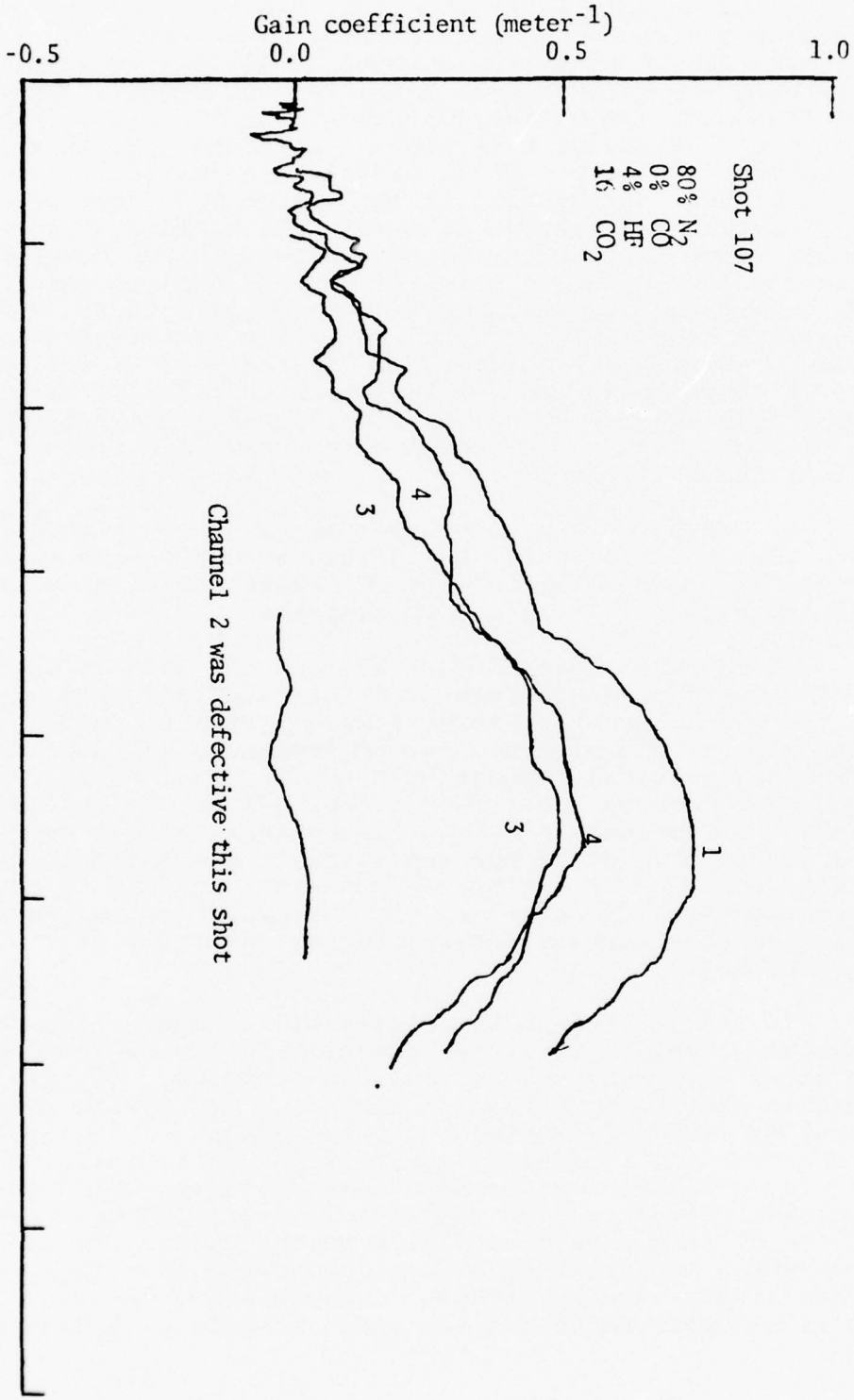

FIGURE 8

Small signal gain versus stagnation pressure.

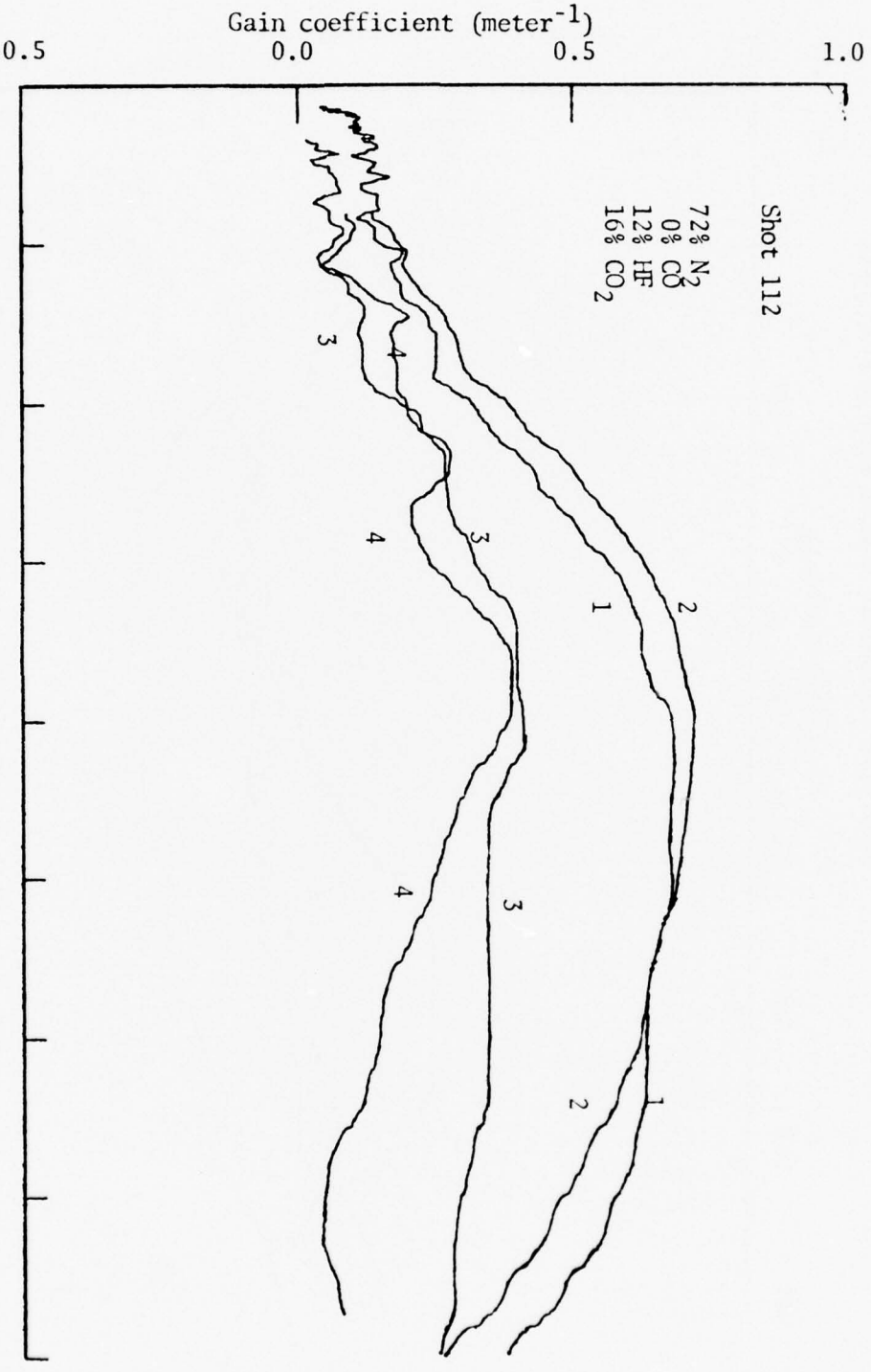

Small signal gain versus stagnation pressure.

FIGURE 9

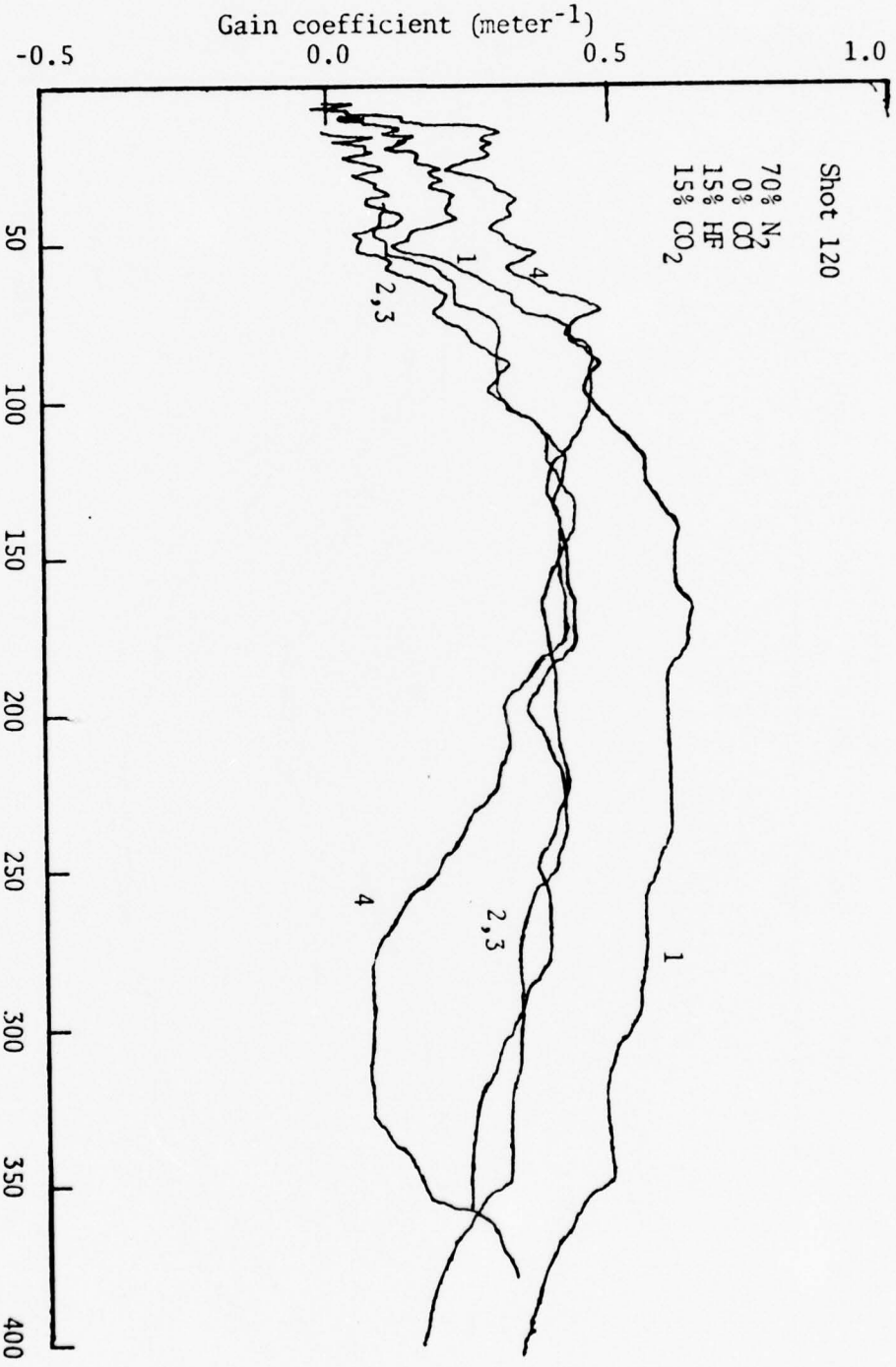

Small signal gain versus stagnation pressure.

FIGURE 10

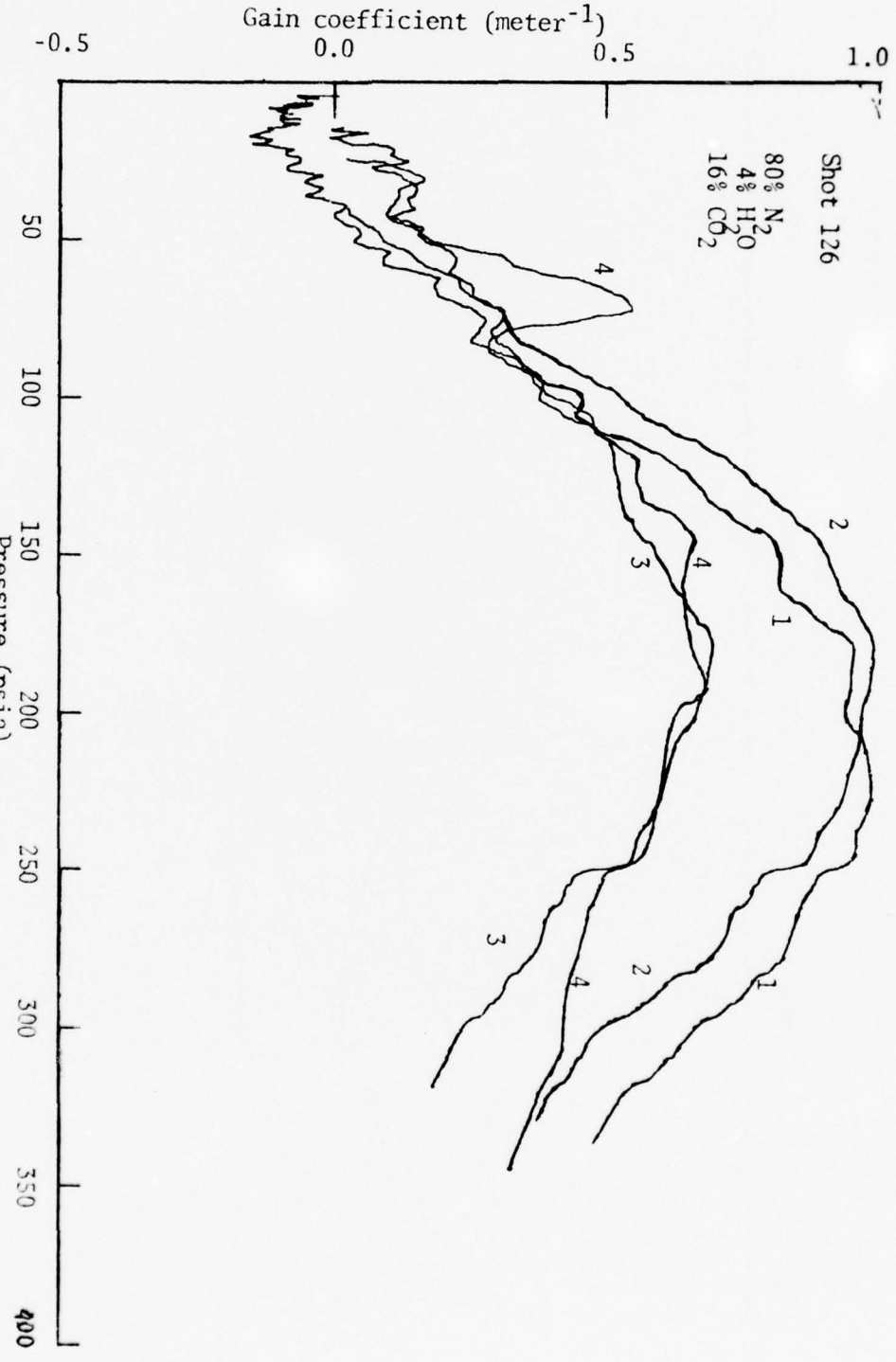

Small signal gain versus stagnation pressure.

FIGURE 11

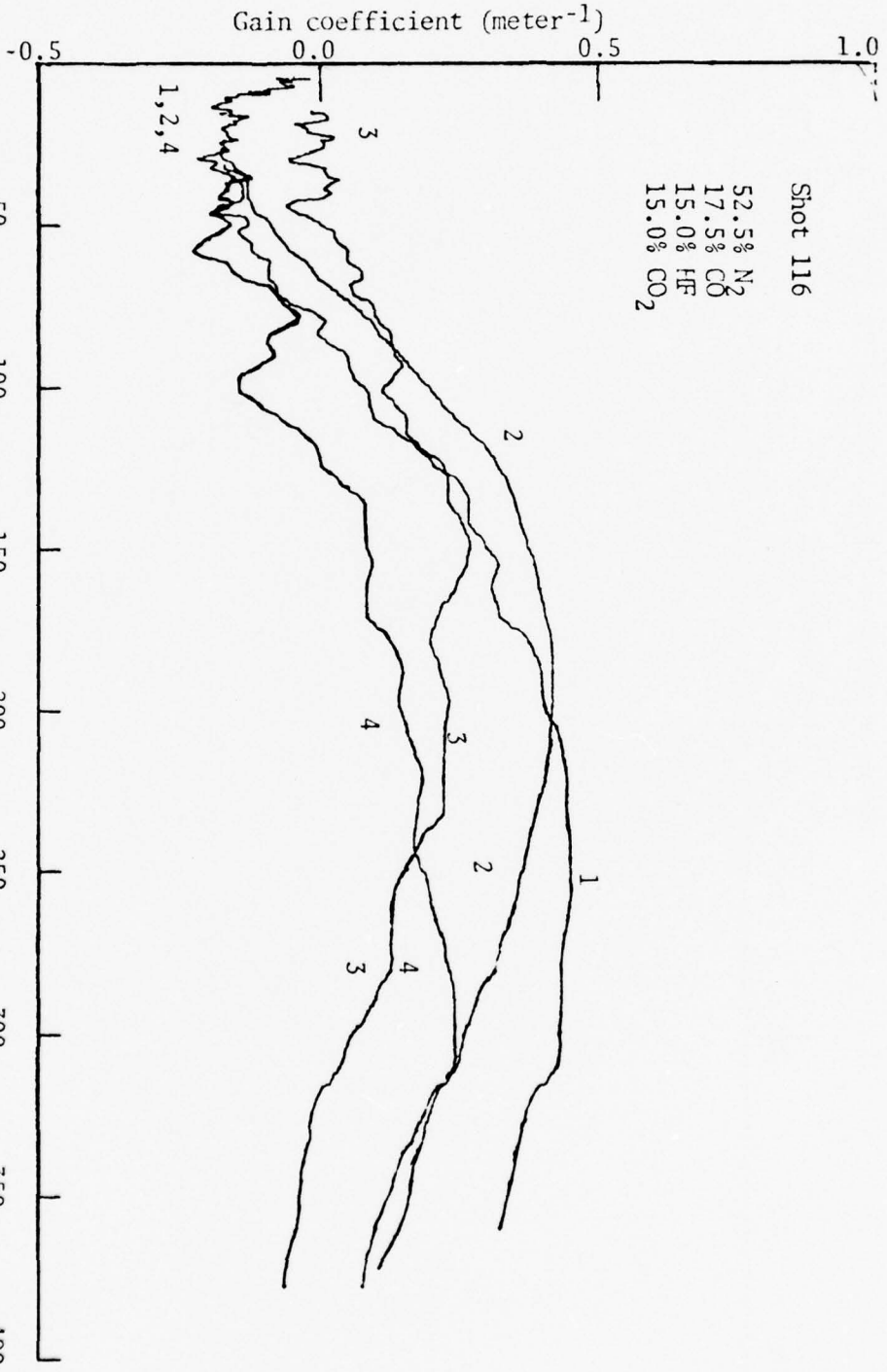

Small signal gain versus stagnation pressure.

FIGURE 12

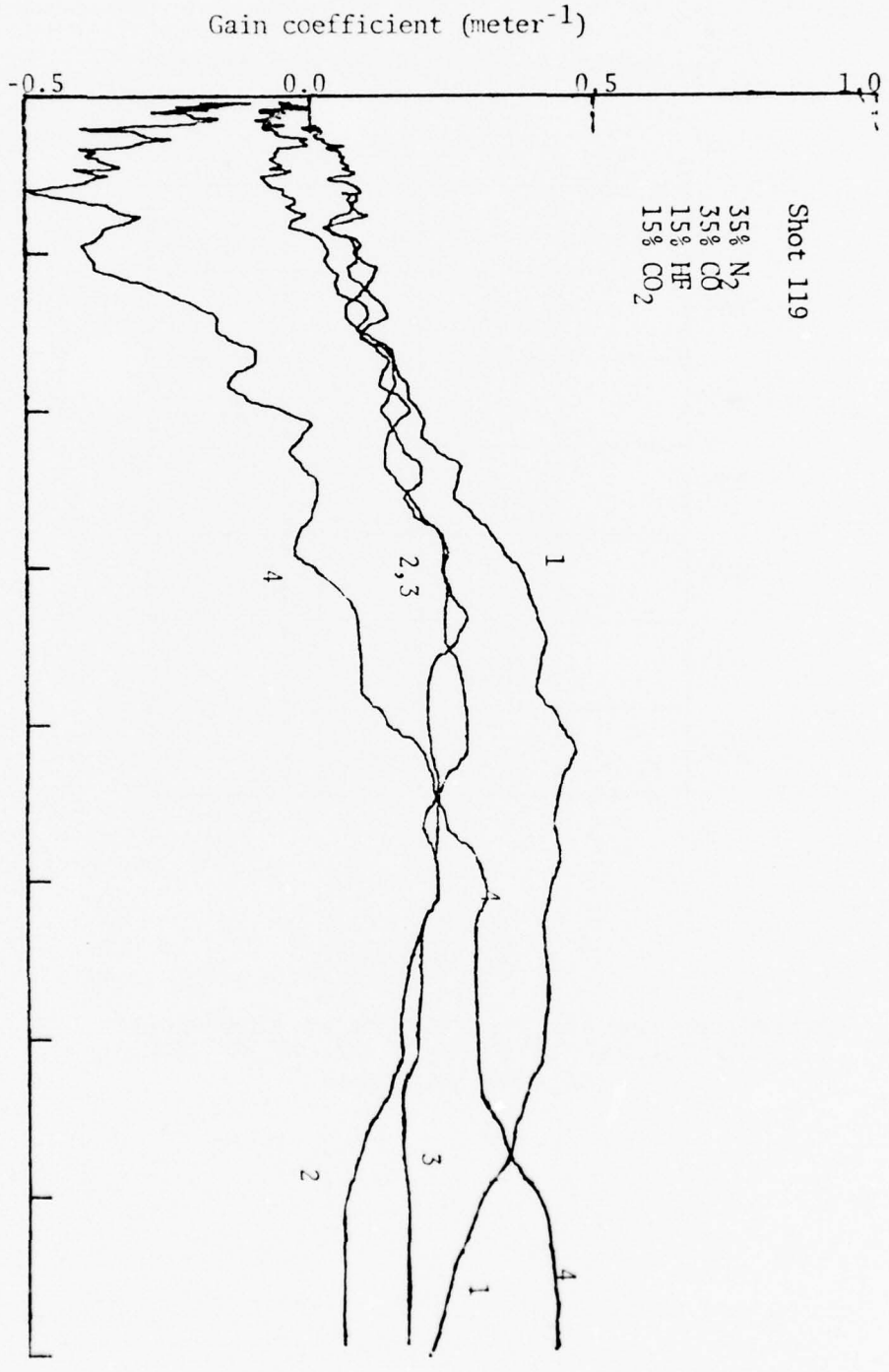

Small signal gain versus stagnation pressure.

FIGURE 13

HCL is the first entry

HF is the second entry

All entries are in units of meter^{-1}

FRACTION OF RELAXATION CATALYST

Fraction of CO to total pumping gas
$CO/(CO + N_2)$

	4%	10%	12%	15%
0%	1.0/.7	.87/X	X/.75	.5?/.7
20%		.8/X		
35%				.7/.43
33%		.8/X		
50%				X/.45
55%		.75/X		
60%	.65/X			

FIGURE 14

Table Entries are Peak Gains at Channel 1
Data Matrix for N_2/N_2 + CO, HF or HCl
CO_2 Gas Mixtures

One entry (0%, CO, 15% HCl) is based on only one shot which was known from spectroscopic gas analysis to have burned incompletely. This entry is followed by a question mark.

This table ignores the behavior of gain with distance downstream. This behavior varies with pressure for any of the mixtures. It is further complicated by the major excursions from a smooth curve which are probably caused by inhomogeneities in the combustion. Nevertheless it is apparent that for almost any mixture there exists a stagnation pressure for which the gain is fairly constant with downstream distance.

The table shows that both HCl and HF behave acceptably with increasing content when no CO is present. However, in combination with carbon monoxide the HF mixture performs poorly. The HCl mixed with CO gives quite good performance. In particular, attention is drawn to the 55% $CO/(CO + N_2)$ and 10% HCl) and 35% $CO/(CO + N_2)$ and 15% HCl mixtures. Extrapolation predicts good results at high CO and high HCl. Evidently HCl is an attractive relaxant the use of which will aid in the formulation of practical condensed phase GDL fuels. Although HF gives poorer results it might still be acceptable in combination with HCl.

6. Some Observations Regarding Gain vs Time Measurements:

The fact that peak gain is achieved when the pressure has dropped to about 50% of its peak value is difficult to explain completely. The effect can also be seen in the gain versus pressure curves. If log (chamber-pressure) is plotted as a function of time (see Figure 17), a straight line should be obtained for a blow-down system with fixed nozzle area. Our plots showed a slight curvature at the higher pressure end indicating a faster than linear change. This non-linear behavior was determined to be caused by loss of gas during solenoid venting. That is, the closing of the solenoid is sufficiently slow so that some of the combustion gas is lost after the diaphragms rupture. The area of the valve opened is about that of the nozzle throat. In addition, the higher initial pressure on the nozzle jaws causes them to spread about 25% in the middle. This spreading also increases the flow rate. This effect was eliminated during that last series of experiments by installing a clamp to provide additional support for the center of the slit nozzle jaws. The extent of the improvement can be seen if the curves for shot 151 (Figures 15, 16, 17) are compared with those taken earlier. Shot 151 is of a 80% N_2, 16% CO_2, 4% H_2O mixture burned with the slit clamp in place and a single diaphragm which was allowed to spontaneously rupture without opening the vent valve.

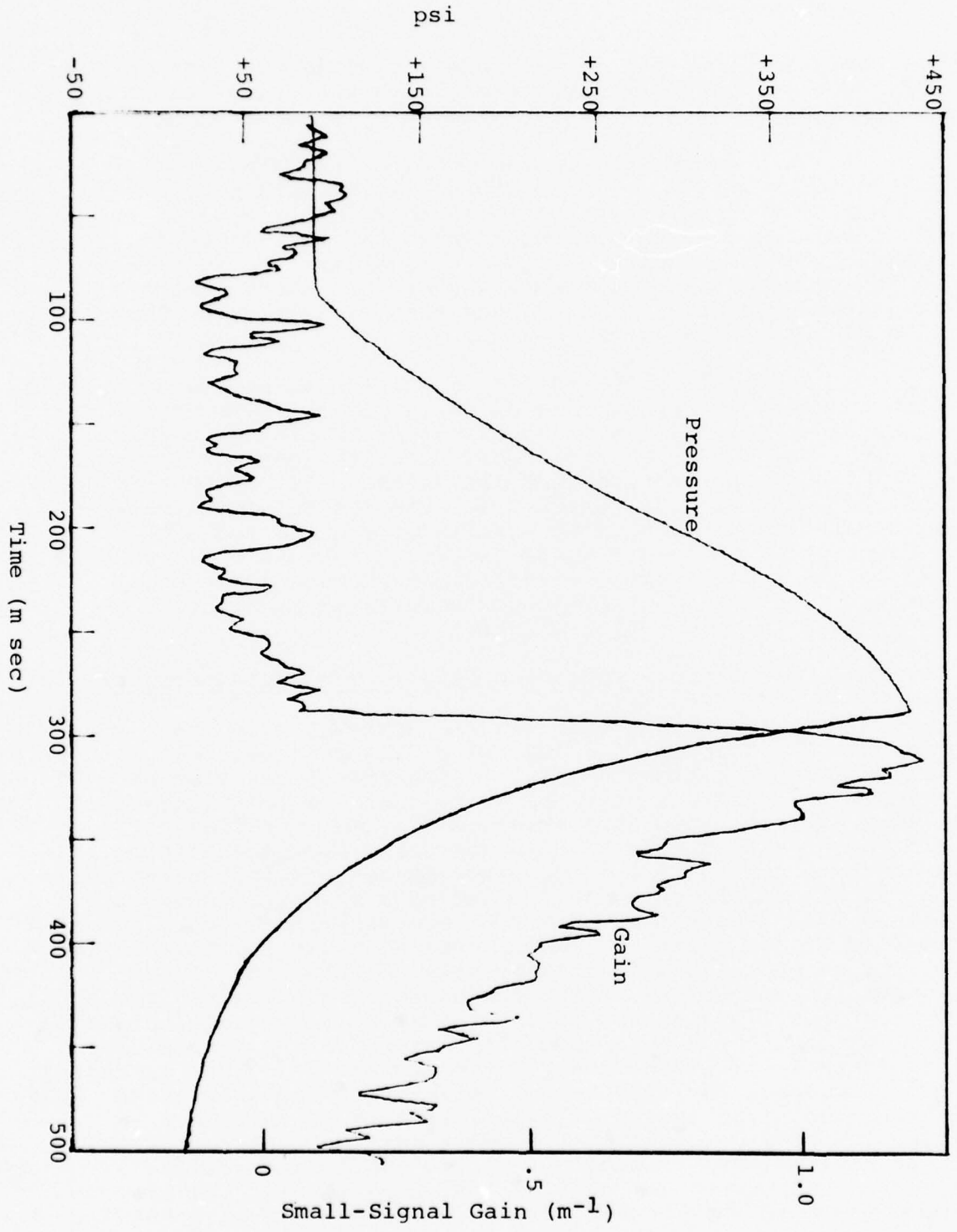

Figure 15

Shot 151 - Pressure and Gain vs Time

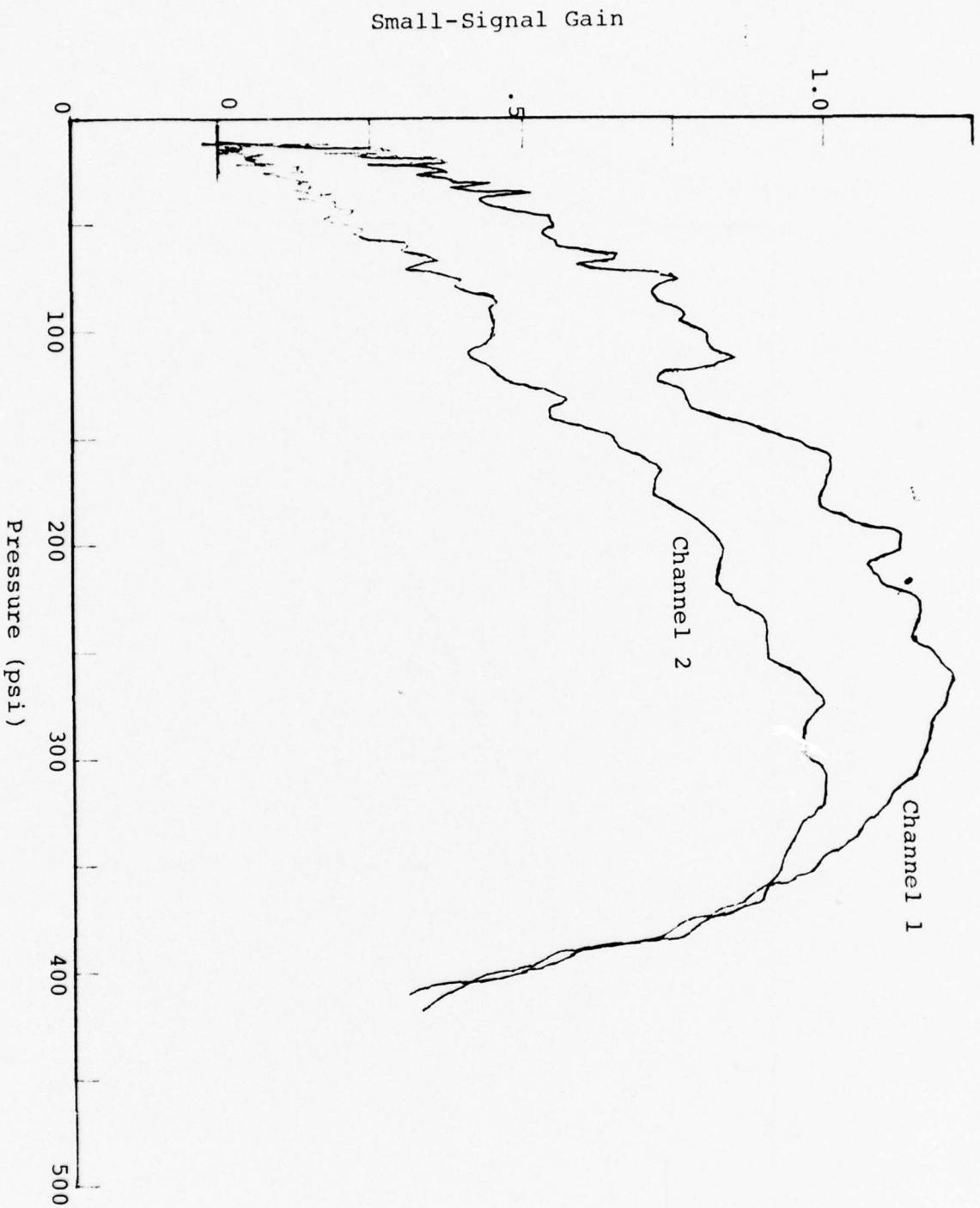

Figure 16

Shot 151 - Small-Signal Gain vs Pressure

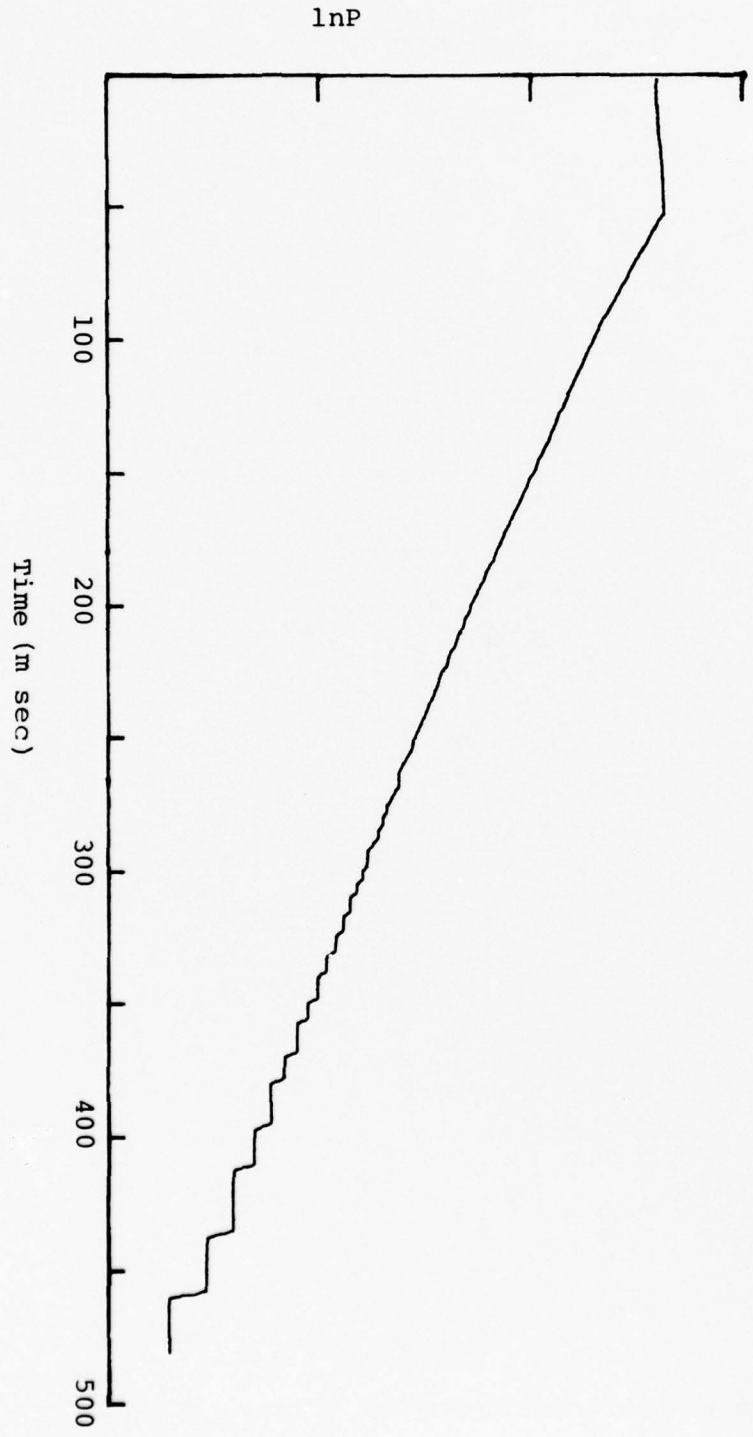

Figure 17

Shot 151 Log e Pressure vs Time

The leveling off and decrease of the gain vs pressure curves as pressure increases is caused in part at least by these conditions specific to our experiment. However, as pointed out by Anderson (reference 1, pp. 13-14), the small-signal gain coefficient is independent of pressure in the pressure region where the line width is determined by pressure broadening. This condition will occur at cavity pressures above 10-20 Torr or chamber pressures above 200-300 psi. At lower pressure, the line width is determined by the doppler effect which depends only on temperature. Here the gain should vary directly with the pressure, i.e. with the number density of CO_2 001 molecules.

IV. Solid Fuel Considerations and Experiments

The gas mixture experiments described above suggest that a useful gain can be achieved from a fuel composition which yields a combustion gas mixture in composition ranges 2-15% HCl, 20-60% CO, 8-16% CO_2 and the balance nitrogen. Since the optimum HCl - containing composition is about 4% HCl, 15% CO_2 and 80% N_2 based on this work, it is clear that the fuel formulator should strive to get as high a nitrogen-content fuel as possible with low hydrogen and carbon contents.

Some examples of possible HCl - yielding solid GDL fuels are given. These examples are based on both previous (1970) work done in this laboratory and our more recent thinking in the light of the HCl/CO series of gain measurements.

1. $C_2N_6O_{12}$ + ½ - CH_2CCl_2- + 7 C (carbon)

   Hexanitroethane (oxidizer); polyvinylidene chloride (binder)

   $\longrightarrow$ 8 CO + $2CO_2$ + HCl + $3N_2$

   57.3% 14.3% 7.1% 21.4%

2. If we replace the carbon by s-tricyanotriazine, C_6N_6 and bitetrazole (m.p. 120°C) to increase the nitrogen content, we can get:

   $3C_2H_2N_8$ + C_2Cl_6 + $-CH_2CCl_2-$ + $3.2C_2N_6O_{12}$

   bitetrazole; hexachloroethane

   + C_6N_6 $\longrightarrow$ $10CO_2$ + 18.4CO + 8HCl + 27.6 N_2

   15.6% 28.8% 12.5% 43.1%

3. Hybrid system (liquid oxidizer, solid fuel)

   9.5 N_2O_4 + ($3C_2H_2N_8$ + C_2Cl_6 + $-CH_2CCl_2-$ + $3C_6N_6$)

   nitrogen tetroxide (liquid oxidizer); Solid

   $\longrightarrow$ $10CO_2$ + 18CO + 8HCl + $30.5N_2$

   15% 27.1% 12% 45.9%

In a practical system, the C_2Cl_6 would be replaced by a halogenated plasticizer.

4. $2C_2N_6O_{12} + 3/2 - CH_2CCl_2 - + 2C_6N_6 \longrightarrow 5CO_2$ (14.7%)

$+ 14CO$ (41.2%) $+ 3HCl$ (5.8%) $+ 12N_2$ (35.3%)

5. $6N_2O_4 + -CH_2CCl_2 - + 3C_6N_6 \longrightarrow 4CO_2$ (12.9%) $+ 16CO$ (51.6%)

$2HCl$ (6.5%) $+ 9N_2$ (29.0%)

In order to plasticize the polyvenylidene chloride, Kel-F oil could be used.

6. $9/4\ C_2N_6O_{12} + 3/2\ C_6N_6 + 2C_2H_2N_8 + -CH_2CCl_2- +$

$-CF_2CFCl -$ (Kel-F oil) $\longrightarrow 5.5CO_2$ (11.8%) $+ 16CO$ (34.2%) $+ 3HF$ (6.4%) $+$

$3HCl$ (6.4%) $+ 19.25N_2$ (41.2%)

Based on these ideas, the following trial solid mixture was selected.

7. $5C_2H_2N_8 + 3.5C_3N_3Cl_3 + -C_2H_{2.25}Cl_{1.75} + 3C_2N_6O_{12}$

Bitetrazole — cyanuric chloride — chlorinated wax (binder) — Hexanitroethane

$\rightarrow$ 10% CO_2 + 28% CO + 16.33% HCl + 45.67% N_2

The cyanuric chloride was substituted for the preferred cyano compound C_6N_6 of Reaction 2, because of the greater safety and stability of the chloride. The above formulation (7) was mixed

and pressed into 2-gram pellets. Since only a limited amount of fuel was available, it was decided to burn six grams per shot. In order to achieve a higher peak pressure, the volume of the combustion chamber was reduced to about a liter with a glass liner. Considerable difficulty was experienced in ignition and in achieving complete combustion. Both ignition and combustion were much slower than the gases, and heat losses were significant. The heat losses were to some extent compensated for and the ignition delay reduced by the lining of the combustion chamber with "heat paper", an ignitor paper which yields no gaseous products. Because of the uncertainties in timing and the limited amount of material available, the solenoid valve was not used to break the diaphragms but they were allowed to break spontaneously. Gain was measured on only two of the trials of this formulation because of the many experimental difficulties. The experimental firing data for the reasonably successful shot (153) are shown in Figures 18 and 19. The pressure-time curve indicates that the diaphragm broke before maximum pressure (complete combustion) was achieved. The burning of the pellets is always quenched by the breaking of the diaphragms. In shot 153, a peak pressure of 219 psia was obtained and a peak small-signal gain of .25 is indicated. The four gain vs pressure curves are plotted one above the other for clarity.

In order to compare the solid fuel with the earlier gaseous fuels on the same basis, a gas fuel, similar in composition to those used earlier, which burned to give the same product gas composition was made up and tested. It gave a peak gain of 0.5/meter. Conclusions: an all-solid GDL laser fuel has been tested to give positive gain. The potential gain of this formulation is 0.5/meter or about 40-50% of the best gaseous systems. The differences between the measured gain (.25/m) and the potential gain are assumed to be specific to the scale and mode of operation of our test laser and are not assumed serious in a longer-burning device with proper fuel grain size and geometry. Some of the ingredients are somewhat volatile, but the storage life at room temperature is good.

The sensitivity, thermal stability and thermochemical data for formulation (7) are shown in Table II.

Further work might usefully be directed toward ingredient selection with the aim of reducing the HCl^- content to 10-12%.

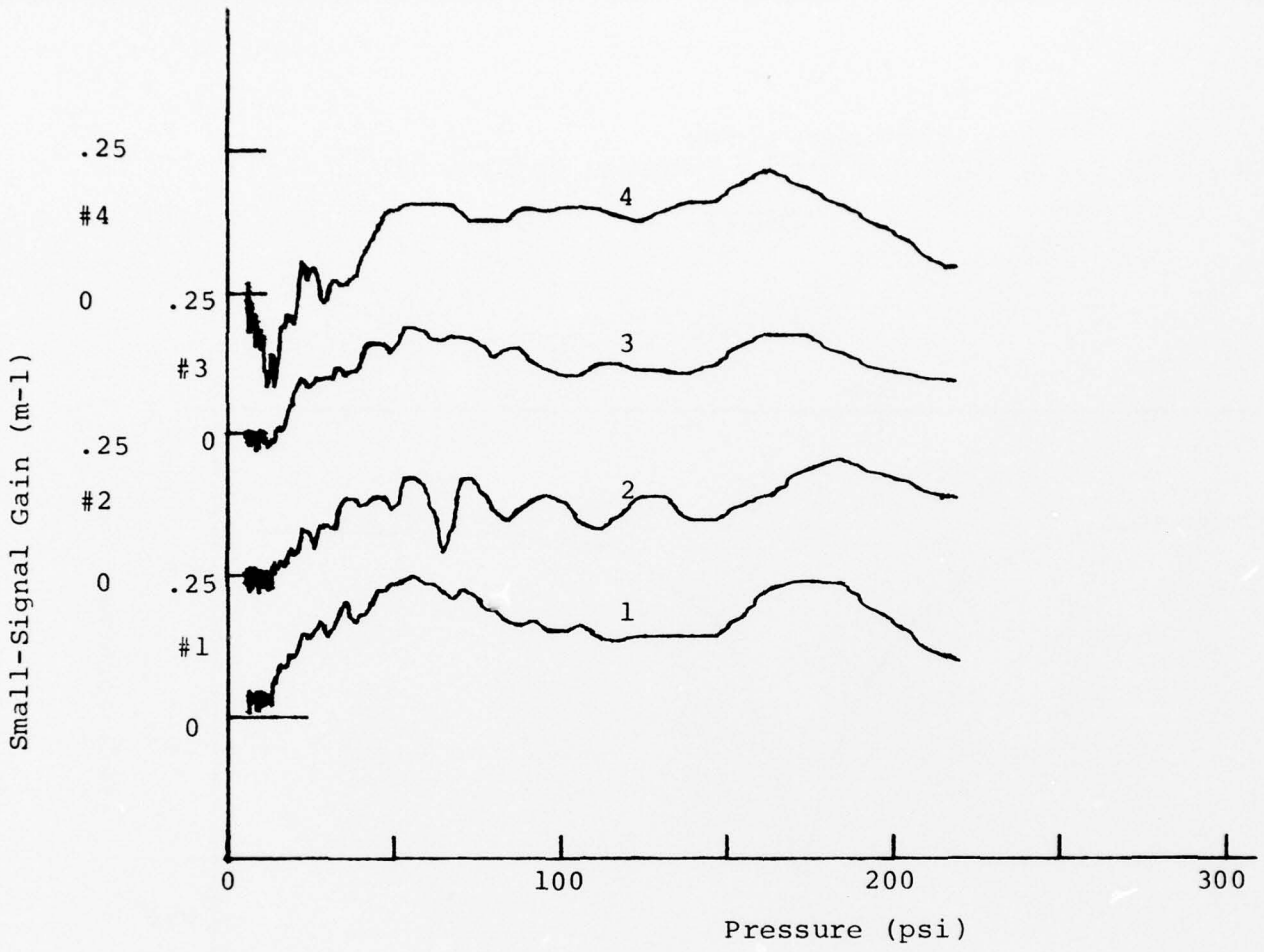

Figure 18

Small Signal Gain versus Stagnation Pressure for Solid Fuel Formulation No. 7 (Shot 153). Channels #1 to #4 Recorded

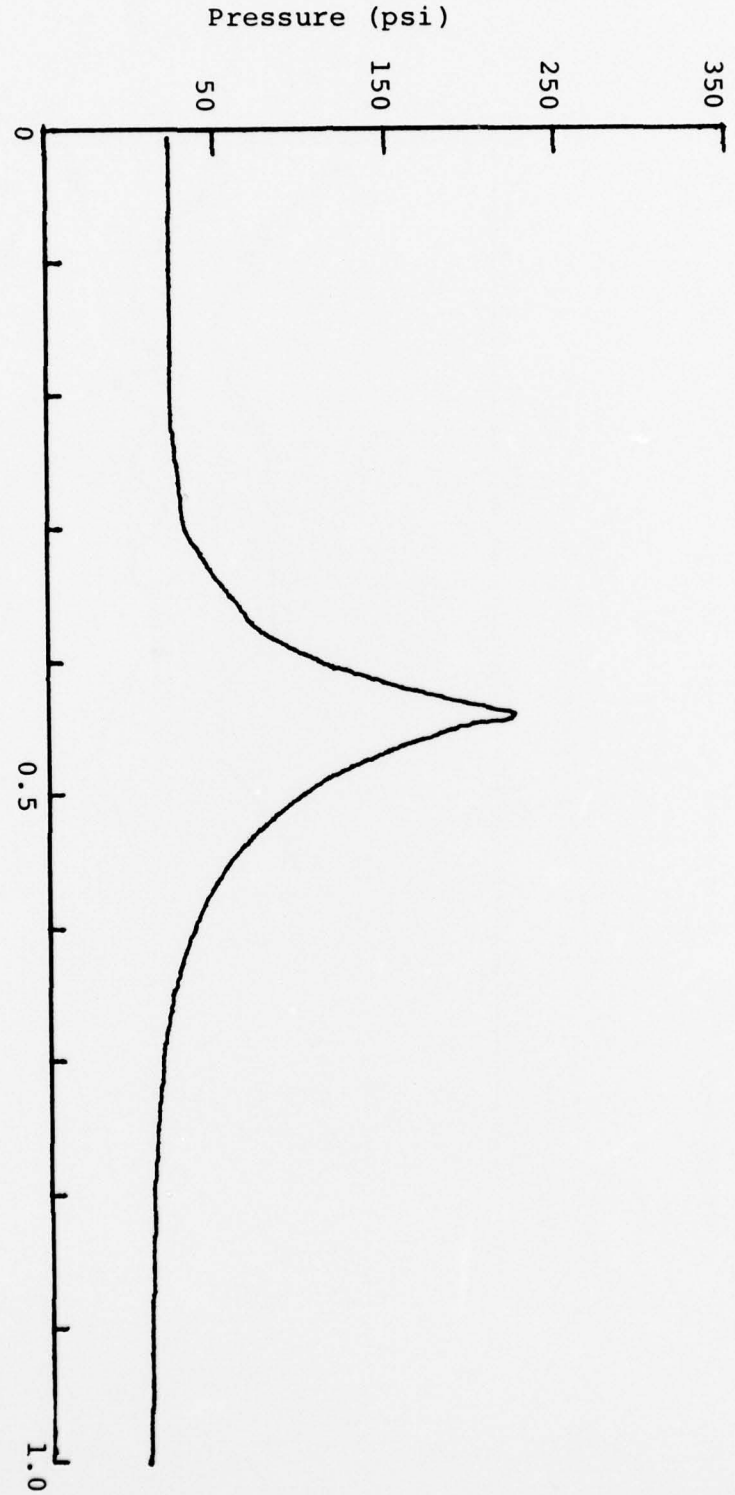

Figure 19

Stagnation Pressure versus Time for Solid Fuel Formulation No. 7 (Shot 153)

Table II

Thermochemical Data for Formulation

Ingredients

Moles	Mass	Theoretical Percentages of Gaseous Products	
$5C_2H_2N_8$	0.59g	CO_2	10.00%
$3.5C_3N_3Cl_3$	0.56g	CO	28.00%
$1C_2H_{2.25}Cl_{1.75}$	0.07g	HCl	16.33%
$3C_2N_6O_{12}$	0.78g	N_2	45.67%

Safety Characteristics:

Impact, 5kg, wgt., 3 consecutive positive, - 75mm
Sliding Friction, 8 ft/sec, 20 trials - 100 lb (til)
Electrostatic, 5000 volts, 20 trails - 0.275 joules (til)
til - theshold initiation level

DTA:

Start of exotherm (^oC) - 80
Ignition temperature (^oC) - 116

$C_2N_6O_{12}$ has a DTA nearly the same as the laser propellant: 82^oC and 117^oC respectively.

V. Mixing GDL Experiments

Several workers have pointed out the advantages of the mixing gas dynamic laser MGDL over the conventional GDL (Ref. 14, 15, 16). In the MGDL, only the pumping gas, e.g. nitrogen, is heated and expanded through the nozzle. The carbon dioxide and relaxation catalyst are injected into the expanding nitrogen stream at points downstream from the nozzle exit. This method has two advantages: First, since the dissociation energies of the usual pumping gases, N_2 or CO, are exceptionally high, high combustion temperatures can be used without loss of efficiency through dissociation. The higher the temperature, the higher the populations of the vibrationally excited pumping gas molecules and the more energy available for pumping the CO_2 lasing level. The second advantage of the MGDL results from the long vibrational relaxation times of the pumping gases. In the absence of the much faster vibrational relaxation rates of the CO_2 and relaxation catalyst, the pumping gas "freezes" at a higher temperature during the expansion, giving again more available energy for laser pumping.

Two serious problems await practical solutions before a useful mixing GDL can be realized. If a combustion MGDL is desired, a fuel problem even more difficult than that of the conventional GDL needs solution. The second problem relates to the minimization of the inevitable thermalization of the vibrational energy when the gases are mixed in the downstream region. The work undertaken here is directed towards the fuel problem.

The fuel problem can be separated from the flow mixing problem, if, rather than measure the small-signal gain in a laboratory-scale MGDL as was done in the conventional GDL fuel study above, we measure the vibrational temperature of the pumping gas after the expansion but before or without downstream injection of the CO_2 and relaxation catalyst. Such a procedure has the additional advantages of allowing us to use our existing laboratory-scale GDL for the MGDL fuel studies.

Three techniques have been considered for the measurement of the vibrational temperature of the pumping gas:

1. Laser Raman technique. The measurements of the vibrational temperature of nitrogen by measuring the relative intensities of the Raman scattered Q-branches of several

vibrational transitions of nitrogen has been achieved by Lapp[5] in flames and gas turbine flows. This method appears to have sufficient sensitivity to determine the vibrational temperature in the low density expanded flow of the MGDL.

2. Dispersive infrared method. Unlike the laser Raman technique, described above, both this infrared technique and the next require at least 5 mol % CO in the pumping gas. Since nitrogen, a homonuclear diatomic molecule, has no infrared spectrum, carbon monoxide, which does, is used to measure vibrational temperatures. A chopped beam of broad-band infrared radiation from a conventional hot infrared source is sent through one of the downstream windows and the absorption of the CO band at 4.7μm measured with a rapid-scanning infrared spectrometer. If the resolution of the instrument is $\sim 1\ cm^{-1}$, the rotational vibrational lines of the v = o to v = 1 and the v = 1 to v = 2 transitions can be separated. The $v = 0 \longrightarrow v = 1$ and $v = 1 \longrightarrow v = 2$, etc. vibrational frequencies are separated because of the anharmonicity of the CO vibrational energy. The relative intensities of these two transitions give directly the relative populations of the two levels or the vibrational temperature of the CO molecule. If we then make the reasonable assumption that CO and N_2 are in thermal vibrational equilibrium, we have determined the vibrational temperature of the pumping gas, CO and N_2. This measurement was tried with a high performance infrared rapid-scanning spectrometer in which a diffraction grating is rotated to achieve the scanning of the spectrum. Because of the low density of CO in the expanded flow, the need for fairly rapid-scanning (~5 msec/CO spectrum) and the consequent poor signal/noise ratio of the measured spectra, no reliable temperature measurements were achieved by this method.

3. Non-dispersive infrared method. This method is similar to the dispersive infrared method above, but has better promise for success because of the much higher signal/noise ratios realizable.

Reference to Figure 20 will make clear the details of this technique. Infrared radiation from a typical incandescent infrared radiation source is chopped at 2-3 kHz and passed through a band-pass filter which passes the frequencies of the rotation-vibration transitions of the CO molecule. The radiation is chopped to distinguish it from that emitted by the CO in the GDL flow. The radiation then passes through the expanded pumping gas just downstream of the nozzle exit where it is partially absorbed by the CO molecules in both the ground and vibrationally excited states.

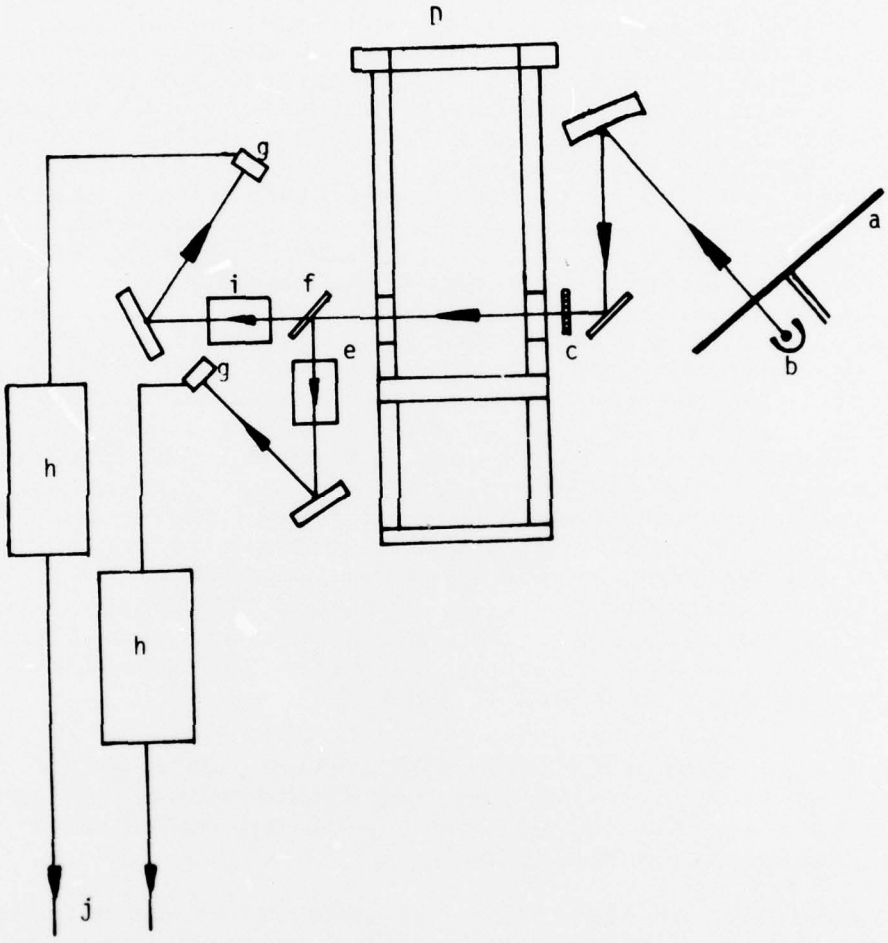

Figure 20: Mixing GDL Test Facility

(a) 3kHz chopper, (b) J.R. source, (c) band pass filter, (d) GDL Test unit, (e) CO cell, (f) beam splitter, (g) detector, (h) lock-in amplifier, (i) reference cell, (j) computer link

After leaving the GDL, the radiation is separated into two beams by a beam splitter. One beam passes through a cell containing CO with about the same rotational temperature as the expanded gas ($\sim 300^{\circ}K$). This vibrationally cold gas absorbs all the beam energy at the $v = 0 \longrightarrow v = 1$ rotational vibrational transitions but hardly any of that at the $v = 1 \longrightarrow v = 2$ transitions ($<10^{-4}$). The detector behind this cell sees only changes in intensity caused by absorption of the excited levels v = 1, 2, etc. but not by the ground state, v = 0. The other beam passes through an empty cell to a second detector which measures changes in absorption by all the populated levels. Analysis of the signals from the two detectors then gives us the desired vibrational temperature. It should be noted that the cold gas filter works well because the GDL gas is vibrationally hot but rotationally cold and the line widths are well matched. The non-dispersive method is promising compared to the dispersive method because of the much higher energy throughput. This advantage chiefly accrues from the fact that in the non-dispersive method we are looking at all times at the total available signal (multiplex advantage) whereas in the dispersive method we need to scan the absorption frequencies and, at any time, the detector sees only a small fraction of the total signal. A further factor of 2-4 is gained by the higher transmission of the non-dispersive optics.

MGDL Fuel Considerations: A problem similar to that encountered in the conventional GDL situation confronts the MGDL fuel formulator. One realizes that the highest performance pumping gas generator will be that which yields the highest nitrogen gas content of the proper temperature. Since no solids are known which give $3000^{\circ}K$ nitrogen with little or no residues or contaminants, the formulator needs to know how far MGDL performance is compromised if some of the nitrogen is replaced by carbon monoxide or if small amounts of relaxants or other contaminants appear in the pumping gas. Our MGDL fuels program is initially directed towards answering these questions. Using the non-dispersive infrared technique to measure the vibrational temperature of the pumping gas and our existing GDL combustion laser test facility, we would examine gas mixtures of various CO/N_2 ratios, with and without small quantities of other contaminants such as CO_2, H_2O, HF, HCl, and products of incomplete combustion. Initial work would be done on mixtures resulting from the burning of cyanogen with oxygen or nitrous oxide with CO mole fractions in the range 0.2 to 0.6. Additions of hydrogen, gaseous organofluorides, or chlorides, etc would serve to generate the desired contaminants.

References

(1) Gas Dynamic Lasers: An Introduction by J. D. Anderson, Jr. Academic Press, New York 1976

(2) Gas Dynamic Lasers, D. A. Russel, Astronautics and Aeronautics, June 1975

(3) CO_2 Mixing Gas Dynamic Laser Incorporating Screen Nozzles, by P. E. Cassady, J. F. Newton and P. H. Rose, Mathematical Sciences Northwest, Inc. AFWL-TR-74-276

(4) Bromfin, B. R., et al,Thermal Laser Mixing in a Highly Convective Flow, Appl. Phys. Letr., Vol 12, No. 8, April 1968, pp. 257-280

(5) J. S. Vamos, AIAA Paper 74-177, 12th AIAA Aerospace Sciences Meeting, Washington D. C., 30 January 1974

(6) R. Tennant, R. Vargas, S. Hardley 12th AIAA Aerospace Sciences Meeting Washington, D. C., 30 January 1974

(7) J. F. Newton and A. L. Pindroh, Mathematical Sciences, Northwest Inc., ACWL-TR-50, June 1974

(8) J. D. Anderson, et al, Population Inversions in an Expanding Gas: Theory and Experiment, NOLTR 71-116, June 1971

(9) S. Yatsin, et al, Pulsed CO_2 Gas-Dynamic Laser, Applied Physics Letters, Vol. 9, No. 3, August 1971

(10) J. Tulip and H. Seguin, Gas-Dynamic CO_2 Laser Pumped by Combustion of Hydrocarbons, Journal of Applied Physics, Vol, 41, No. 9, August 1971

(11) J. Tulip and H. Deguin, Explosion-Pumped Gas-Dynamic CO_2 Laser Applied Physics Letters, Vol. 19, No. 8, October 1971

(12) J. S. Vamos, Naval Surface Weapons Center, WOL, MD, Unpublished Data, Private Communication 1974

(13) R. A. Tennant, R. Bargas, W. B. Watkins and S. G. Hadles, Air Force Weapons Laboratory, Kirtland, NM AFW-TR-73-273

(14) Bromfin, B. R., Boedeker, L. R. and Cheyer, J. P., "Thermal Laser Excitation by Mixing in a Highly Convestive Flow", Appl. Phys. Letter 16 214-217 (1970).

References (cont)

(15) (a) Taran, J. P. E., Charpend, M. and Barghi, R., "Investigation of a Mixing CO_2 GDL", AIAA Paper No. 73-622(1973)

(b) R. Borghi, A. F. Carega, M. Charpenel and J. P. E. Taran, "Supersonic Mixing Nozzle for Gas Dynamic Lasers", Appl. Phys. Letter 22 661 (1972)

(16) P. E. Cassady, J. F. Newton, P. H. Rose, "CO_2 Mixing GDL Incorporating a Screen Nozzle", Mathematical Sciences Northwest, Inc. Final Report to the Air Force Weapons Laboratory AFWL-TR-74-276 (August 1975).

(17) M. Lapp. "Flame Temperatures From Vibrational Raman Scattering", in "Laser Raman Gas Diagnostics", M. Lapp and C. M. Penney, editors, Plenum Press, New York (1974).

(18) J. L. Wagner and John D. Anderson, Jr., "Effect of Nozzle Throat Radius of Curature on Gas Dynamic Laser Gain", J. Spacecraft and Rockets, 9 (6) 471 (1972).

(19) R. A. Greenberg, A. M. Schneiderman, D. R. Ahouse and E. M. Parmentier, "Rapid Expansion Nozzles for Gas Dynamic Lasers", AMP 314, AVCO Evertt Research Laboratory, December 1970.

DISTRIBUTION

Naval Air Systems Command
Attn: AIR-310
Washington, D. C. 20361 1

Naval Material Command
Department of the Navy
Washington, D. C. 20361
HEL Project Office, MP-22-20 1

Naval Material Command
Department of the Navy
Washington, D. C. 20361
HEL Project Office, PM-22-50 1

Office of Naval Research
Attn: ONR-421
800 North Quincy St.
Arlington, VA 22217 1

U.S. Air Force
Kirtland AFB, NM87116
Attn: Capt. Hemm AFWL/LRL 1

Air Force Rocket Propulsion Lab.
Edwards, CA 93523
Attn: LKCB 1

Naval Sea Systems Command
Attn: SEA-0331
Washington, DC 20362 1

Naval Weapons Center
Attn: Code 753 - Tech. Library
China Lake, CA 93555 2

Naval Postgraduate School
Attn: Library, Tech. Repts.
China Lake, CA 93555 2

Naval Research
Attn: Code 473, Power Branch
800 N. Quincy St.
Arlington, VA 22217 1

Naval Sea Systems Command
Attn: SEA-09G32
Tech. Library
Washington, DC 20390 2

Naval Ordnance Station
Attn: Code 613
Technical Library
Indian Head, MD 20640 3

Naval Sea Systems Command
Attn: SEA-03B
Washington, DC 20360 1

Headquarters
Air Force Special Communications Center
USAFSS
San Antonio, TX 78243 1

Defense Documentation Center
Cameron Station
Alexandria, VA 22314 12